Classification of Colored Retinal Images for Diabetic Retinopathy Based On HOG Feature Selection.

Thesis submitted in partial fulfillment of the requirements for the award of degree of

Master of Technology

In

Computer Science and Applications

Submitted by

Rachik Raj Sharma

Roll No. 601534011

Under the supervision of:

Dr. Husanbir Singh Pannu

Lecturer, CSED Department.

COMPUTER SCIENCE AND ENGINEERING DEPARTMENT

THAPAR UNIVERSITY

PATIALA – 147004

June 2017

CERTIFICATE

I hereby certify that the work which is being presented in the thesis entitled, "*Classification Of Colored Retinal Images For Diabetic Retinopathy Based On HOG Feature Selection*", in partial fulfillment of the requirements for the award of degree of Master of Technology in *Computer Science and Engineering* submitted in Computer Science and Engineering Department of Thapar University, Patiala, is an authentic record of my own work carried out under the supervision of *Dr. Husanbir Singh Pannu* and refers other researcher's work which are duly listed in the reference section.

The matter presented in the thesis has not been submitted for award of any other degree of this or any other University.

(Rachik Raj Sharma)

This is to certify that the above statement made by the candidate is correct and true to the best of my knowledge.

(Dr. Husanbir Singh Pannu)

Assistant Professor, CSE

Department

ABSTRACT

Diabetic Retinopathy is an eye disease that affects the people suffering from diabetes. The high sugar levels in blood leads to damaged blood vessels in eyes. Diabetic retinopathy is one of the major causes of blindness in present day. Diabetic retinopathy is mainly identified by red spots known as micro-anuerysms and bright lesions called exudates. It has been seen that the early detection of diabetic retinopathy is done mainly by identifying these exudates. Therefore an automated early detection of diabetic retinopathy is need of the moment. Inspired by this manifestation of the exudates in the eyes of person suffering from diabetes, a framework is proposed for the early detection of diabetic retinopathy. In this research we consider the colored retinal images of the eyes taken by fundus camera. The proposed system performs the feature extraction on the retinal images after the preprocessing stage. The features are extracted by HOG technique. Finally, the classification for normal and abnormal retinal images is done by using well trained KNN, SVM and Random Forest. Ensemble model of the three classifiers namely, KNN, SVM and MLP is also used for achieving a better accuracy. This approach is evaluated on 400 colored fundus images, including two publically available dataset. The accuracies of 89%, 87%, 95% and 93% are obtained for the three individual classifiers and the ensemble model respectively.

TABLE OF CONTENTS

LIST OF FIGURES

LIST OF TABLES

ABBREVIATIONS

CAD	Computer Aided System
DR	Diabetic Retinopathy
ARMD	Age Related Macular Edema
OD	Optical Disc
PC	Personal Computer
HOG	Histogram of Gradients
SURF	Speeded Up Robust Features
SIFT	Scale-Invariant Feature Transform
ANN	Artificial Neural Network
GMM	Gaussian Mixture Model
SVM	Support Vector Machine
KNN	K-Nearest Neighbors
SVR	Support Vector Regression
XML	Extensible Markup Language
CSV	Comma Separated Values
MLP	Multilayer Perceptron

CHAPTER 1

INTRODUCTION

Diabetic Mellitus, commonly known as diabetes, is described by the World Health Organization as a lifelong disorder that is caused by high sugar levels in the blood. It is classified into two types, Type I (insulin dependent diabetes) and TypeII (non- insulin dependent). The Type I diabetes is caused when the pancreas fails to produce sufficient insulin. Type II diabetes is caused by metabolic disorder that result in condition in which the blood cells are incapable of using the insulin properly. This condition ultimately result in lack of insulin in body.

Insulin is the hormone released by pancreas. The beta cells in pancreas are responsible for the production of insulin and it works by regulating the blood sugar levels. The stage where the sugar level in blood crosses a threshold value it results in serious damage to the body's metabolism system. This stage is called hyperglycemia and is also one of the main reasons for the diabetic retinopathy. Increase in age and weight, sedentary lifestyle are two basic causes for diabetes mellitus.

Amid the initial two years of infection, roughly all patients with insulin dependent diabetes and more than 50% of patients with non-insulin dependent diabetes have retinopathy [1]. The predominance of diabetes is evaluated to increment from 2.7% to 4.5% in the time traverse of 2000−2030. The aggregate number of individuals is anticipated to rise from 160 million of 2000 to 350 million of 2035 [2]. Diabetic patients can forestall serious visual misfortune by going to general diabetic eye screening programs and getting ideal medications.

Diabetic retinopathy (DR) and age related macular degeneration (ARMD) are among the main reasons for visual debilitation around the world. DR happens most much of the time in grown-up matured (18−75) years, and it is described by the nearness of red sores (microaneurysms) and brilliant injuries (exudates) which show up as little white or yellowish white stores with sharp edges and variable shapes situated in the external layer of the retina, their location is fundamental for diabetic retinopathy screening frameworks. ARMD generally influences individuals more than 50 years old.

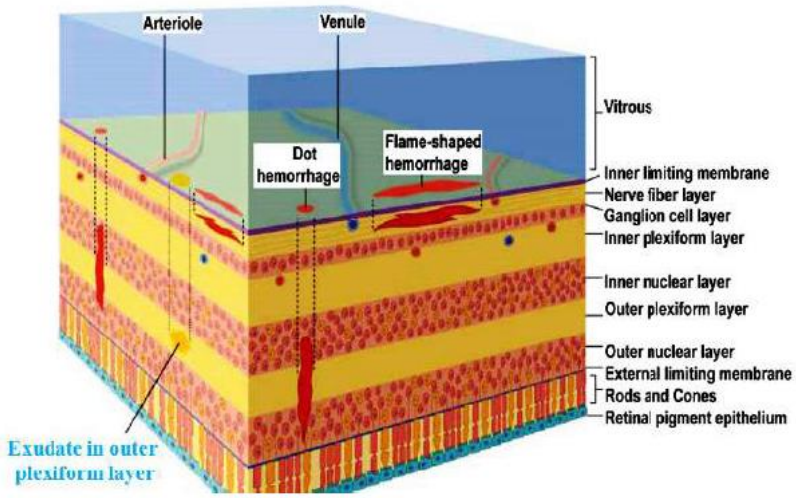

Figure 1.1 : Example of exudates in the retinal layer of eyes[1].

It is caused by a harm to the macula, the little touchy territory of the retina that gives focal vision (seeing fine points of interest and hues), and sorted by drusen, small yellow or white stores in a retina layer called Bruch's film. The Severity of ARMD can be sorted into three classes: early, middle of the road, and progressed. Three cases of exudate, drusen and optic disc in a human retina are shown in Figure 1.1, Figure 1.2 and Figure 1.3 individually.

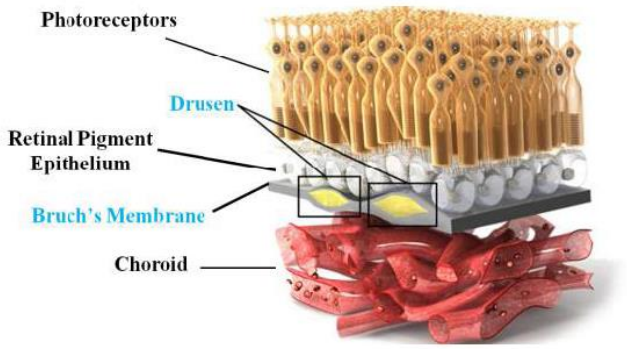

Figure 1.2 : Example of drusen in retinal layer of eyes[1].

These bright lesions also called as exudates in medical terminology are caused when the blood vessel that are large in size in the eyes gets blocked due to the increased sugar level. The body reacts to this damage by trying to develop new blood vessels. The new vessels tend to be weak and grow in random wrong locations. These new vessels thus are unable to restore the proper vision function. The exudates are the result of breakdown of the retina barrier. This allows the proteins and lipid to leak through the broken patches. The exudates thus are granular, yellow spots. These can be classified

broadly into two categories: hard exudates and soft exudates(cotton wool spots). The hard exudates are caused by the severe leakage of the proteins and lipid, while the soft exudate are responsible for the damage to the nerve fiber and are whitish-yellow in colour.

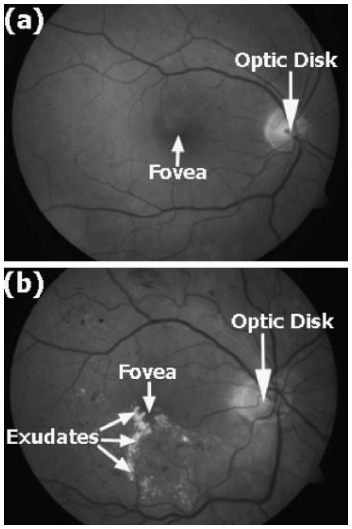

Figure 1.3: Similarity in optic disc and exudates in retinal images of eye[2].

The early detection of the the exudates in the retinal images of the eye is crucial for the prevention of the vision loss in diabetic patients. More specifically, the manifestation of the hard exudates are the only early prevalent signs for the detection of the disease[1]. Further the non-homogeneous illumination, lack of contrast and the varialtion in the colour in the retinal images adds to the challenge of CAD systems to recognize these hard exudates accurately. An automated system will help to save a lot of effort and time in screening coloured retinal images. A lot of attempts have been made to succesfully empower the CAD systems for correct screening of the retinal images.

In many patients suffering from diabetes the exposition of the bright lesions such as exudates can be the only early signs for the diabetic retinopathy. Many attempts have been made to use computer aided detection (CAD) systems for detecting the presence of the exudates in the eye of the diabetic person. The similarity in physical characterstics of the bright lesions with the other lesions like drusen and other parts of eye like optic disc makes it difficult for the computer aided detection (CAD) systems to correctly identify the exudates and thus the early diabetic retinopathy. This is a challenge for the CAD systems. Thus developing a automated system to examine and

study the coloured retinal images will help the opthamologists to correctly identify the exudates and will decrease the false negative rates.

1.1Aims And Objectives

In this research we consider the coloured retinal images of the eyes taken by fundus camera. Image pre-processing is done first to detect the exudates (bright lesions) in the retina. The proposed system performs the feature extraction on the retinal images after the pre-processing stage. The features are extracted by approaches like HOG. Finally, the classification for normal and abnormal retinal images is done by using well trained neural network, SVM and Random Forest. Ensemble model of the three classifiers is also used for achieving a better accuracy. This approach will be evaluated on large dataset of coloured fundus images, including publically available dataset MESSIDOR[41]. This automated process will save the manual work and time of the ophthalmologist. This will also achieve better accuracy.

The objectives of the current research work can be listed as:

1). To study, analyze and explore the already existing detection methods for non-proliferative and proliferative diabetic retinopathy in retina using current fundus imaging procedures and identifying gaps and limitations in the manual procedures and existing automated detection systems proposed so far.

2). To propose an automated detection system to identify the lesions in the retina of a diabetic eye by employing feature extraction and feature ranking. Then classifying the coloured retinal images by using the ensemble of existing classifiers models.

3). To test and validate the proposed technique on publically available datasets of fundus images and on images collected in real time using various standard metrics subjectively and quantitatively with other state-of-art procedures.

1.2 Thesis Structure:

1. **Chapter 1** introduces the subject area of the thesis research and provides an overview of the need and importance of the problem.

2. **Chapter 2** defines the basic anatomy of the human eye. The main features of the eyes affected by the diabetic retinopathy. Different types of lesions are explained including the ones responsible for the identification of the diabetic retinopathy. The different satges of Type 1 and type 2 disease are explained.

3. **Chapter 3** covers a detailed literature review of the different methodologies followed till date to identify different lesions in the retinal image of the human eye. The algorithms to classify the normal and abnormal retinal images are also reviewed in detail.

4. **Chapter 4** gives an insight into the methodology followed in this reaserch work. It includes preprocessing, feature extraction and ranking and classification by ensembled models.

5. **Chapter 5** provides and discusses results.

6. **Chapter 6** concludes the work done in this research and provides the reccomendations for the future work.

CHAPTER 2

BACKGROUND

2.1 Eye Anatomy

Human eye is the most valuable and sensitive organ and natural optical instrument in the human body. It is located close to the brain so that its messages could arrive quickly. Its primary function is to detect visible light whose wavelengths ranges from 400 to 700 nm [1].

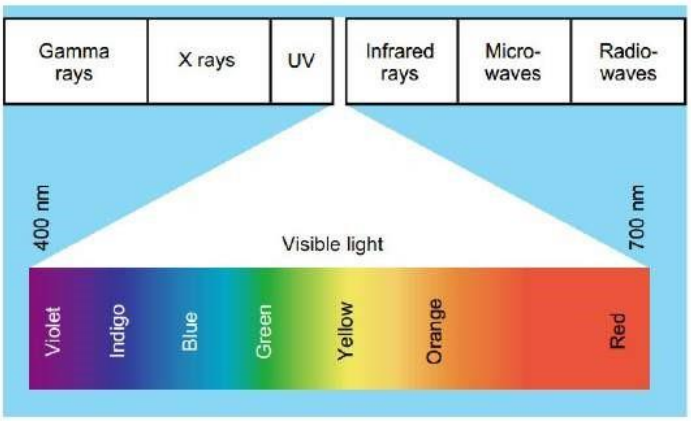

Figure 2.1: Electromagnetic spectrum [2].

Human eye enables us to see the beautiful colorful world around us. It can differentiate almost 10 million colors and capable of detecting single photon. A human eye is very much similar to camera, far more than just the ability to capture images. Camera and the human eye does have some similarity. Your eye, has an incredible flexible lens that allows you to see very close and far away objects whereas a camera would require multiple lenses to accomplish that kind of versatility. The image captured by camera are permanent. Your memories of what you see are not only fluid and ephemeral, they are colored by your own memories of the events and your feelings and expectations.

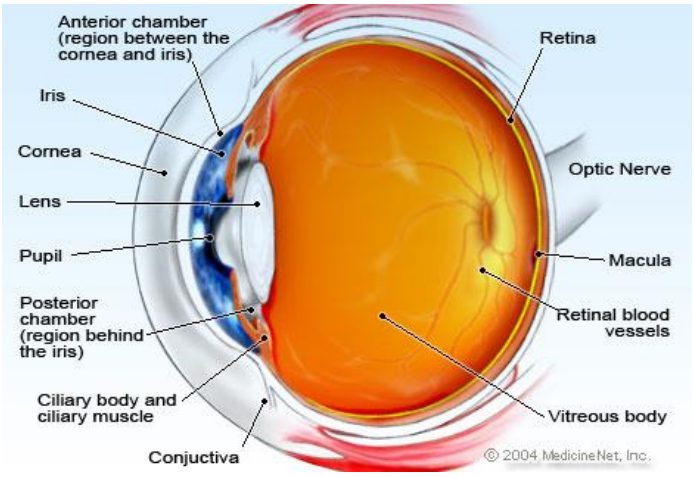

Figure 2.2: Detail illustration of human eye [2].

Figure 2.2 shown above represents a cross section of human eye anatomy. Functioning of eye is very complex as it requires involvement of small and intricate parts. Light enters through cornea, which is a clear surface of the eye. The cornea refracts or bend light onto the lens. Iris is the colorful part of the eye which surrounds the pupil and itself is covered by Cornea. Iris controls the amount of light entering the eye by changing the size of the pupil. The shape of the lens is changed with the help of auxiliary muscles and the object is bought into focus and also improves the already refined image. The lens focuses light onto retina that starts the translation of light into vision [3]. In this research work, the function of retina will be our main areas of research, hence it will be elaborated in depth.

2.1.1 Retina

Retina is that part of the eye which plays a significant role in vision. It is located at the back of the eye and contains light sensitive tissue. Retina has millions of photosensitive cells commonly known as photoreceptors. These photoreceptors are light sensitive which converts light rays into electrical signals. The main purpose is to receive light and convert it into neutral signals and send these signals to brain for visual recognition through the optical nerve fibers. Photoreceptors consists of two major structures commonly known as rods and cones. A basic difference between rods and cones is shown in the Table 2.1.

Table 2.1: Rods and Cones.

Rods	Cones
Responsible for detecting the dim lights to generate signals	Responsible for detecting bright light with color to generate signals
Approximately 125 million rods cells	Approximately 6 million cones cells
It is located in the peripheral retina	Found in highly sensitive part macula which is responsible for visual acuity
Acromatic and night scotopic vision	Chromatic and Photopic vision

The retina is divided into many distinguishable layers as shown in the Figure 2.3

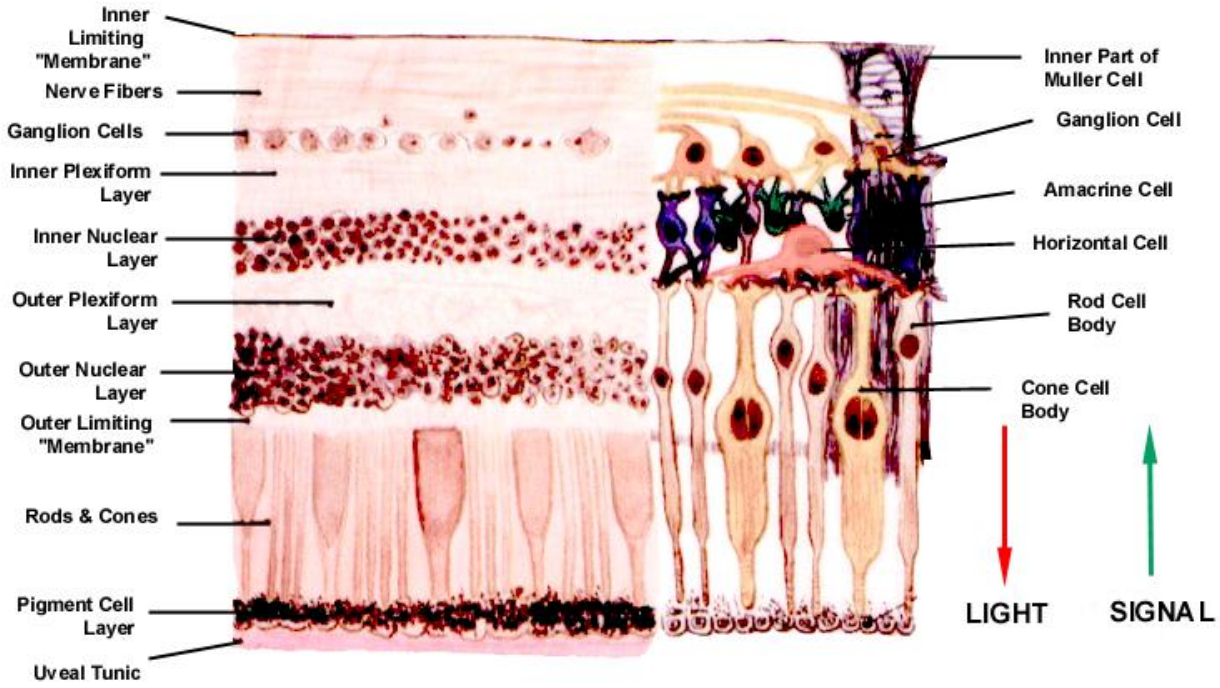

Figure 2.3: Schematic view of retina layers organization [3].

The different layers of retina are organized as follows:

1. The Inner Limiting Membrane (ILM) – It formed by astrocytes and located between the retina and the vitreous body.
2. Ganglion Cell Layer (GCL) – It is a layer that consists of displaced amacrine cells and retinal ganglion cells.
3. Inner Plexiform Layer (IPL) – This layer is the interaction point of bipolar, amacrine and ganglion cells.
4. Inner Nuclear Layer (INL) – It is a layer of inner granules containing cell bodies of bipolar, amacrine and horizontal cells.
5. Outer Plexiform Layer (OPL) – It consists of dense network between dendrites of horizontal cells and photoreceptor cell.
6. Outer Nuclear Layer (ONL) – Outer most layer of retina which contain cell bodies of rod and cone photoreceptors.
7. Outer Limiting Membrane (OLM) – It maintains the structure of the retina through mechanical strength.
8. Photoreceptor Layer - It contains the inner and outer segment of photoreceptor.
9. The Pigment Epithelium Layer – It is commonly known as RPE that is located outside retina and attached to choroid. Nutrients like glucose, retinol and fatty acids are absorbed by RPE and later delivered it to photoreceptors.

The ganglion cells are a type of neurons that receives visual information from photoreceptors through horizontal and amacrine neurons.

2.2 Retinal Imaging Techniques

Retinal Images are visualized through fundus camera that captures the back of eye. There are certain disease that manifest themselves within retina which are diagnosed through Retinal Imaging Techniques. Diabetic retinopathy, glaucoma, and age related muscular degeneration are such eye diseases. In the mid of 21st century, ophthalmoscopy, fluorescein angiography, fundus photography, and diagnostic ultrasound were considered the only retinal imaging modalities. Techniques like indocyanine angiography, infrared imaging, optical coherence tomography (OCT), and scanner laser ophthalmoscopy (SLO) have been recently introduced in the world of Retinal Imaging. In addition to this, data processing and storage are permitted through digital technology [3].

Figure 2.4: Examples of retinal images; (a) Healthy, (b) Diabetic retinopathy, (c) Age related macular degeneration, (d) Glaucoma retinal images [3].

The health of the retina and vitreous humor is determined by ophthalmoscopy or fundoscopy. There are two types of examinations performed in ophthalmoscopy: direct and indirect. The first tool is about the size of a small flashlight with many flashlight that can magnify up to 15 times. The second tool is a handheld lens and slit lamp microscope is attached to a headband.

Fundus Photography is used to record color images of the interior surface of the eye that includes the retina, retinal vasculature, macula, posterior pole, macula, and optic disc through the diluted pupil of the patient that enhances the quality of image. Specialist or trained medical professionals helps in transfer of images via networks for remote viewing. In addition, it documents conditions diabetic retinopathy and vision deterioration that leads to blindness. A fundus camera has a low power microscope that is attached to a camera which provides magnified views of the fundus. A normal angle of view is 30^{o} that creates a film image of 2.5 times larger than life. Less magnification images are captured by wide angle fundus camera whose angle lies between 45^{o} and 140^{o}. Whereas, 20^{o} or less angle of view [2] are among the narrow angle fundus camera. Figure 2.4 shows different examples of retinal fundus camera.

According to [4], fundus imaging is a process that involves 2D representation of the 3D retinal structures projected onto the image plane. In Table 2.2 techniques/modalities belonging to fundus imaging are grouped together.

Table 2.2 Different fundus imaging modalities[4].

Name	Description
Fundus Photography	Performs to evaluate the abnormalities in the fundus, follow diseases progress and thereon plan the treatment accordingly. At specific wavelength, intensities of image corresponds to reflected light which includes red free.
Color Fundus Photography	Full examination of the retina in color by means of white light illumination. Subsequently, intensities of image represent the amount of reflected red, green and blue wavelengths.
Stereo Fundus Photography	Exploitation of two or more view angles estimates the depths.
Hyperspectral Imaging	It produces multiple specific wavelength bands. Oxygen consumption in the retina is monitored that indicates potential diseases.
Scanning Laser ophthalmoscopy	Sharp retinal images are provided by single wavelength laser light which reaches the surface of the retina and records its surface details.
Adaptive Optics Scanning Laser Ophthalmoscopy (AOSLO)	Correction of optical light by modeling the deviation in its wave front.
Fluorescein Angiography	Intensity of image constitutes the amount of emitted photons from photosensitive material i.e. fluorescein or indocyanine

green fluorophore injected into the patient blood stream.

Ophthalmic ultrasound is very much essential as it is helpful in diagnosing retinal detachment, tumors, vitreous bleeding, lesions in the eye socket bone, or foreign bodies in the eye. This technique is similar to ultrasound which is used to scan different body organs of human body, sound waves are sent from a probe placed on the eye to provide sonar images of inside of the eye.

Optical coherence tomography is a micron resolution cross-sectional study of retina. It is based on low-coherence interferometry in order to measure the echo time delay of the back scattered light in the sample as A-Scan ultrasound acquisition. OCT is typically based on principle of michelson interferometry. A low-coherence infra-red light split into two disjoint paths and is directed through the ocular media to the retina and a reference mirror. Light from both beams are then reflected and overlap within a fiber-optic infer meter [4]. An OCT image of a normal human macula is shown in the Figure 2.5.

2.3 Clinical Lesions of the Retina

In this section two groups of retinal diseases are discussed: yellow white spots and red white spots. The former includes cotton wool spots, drusen and hard exudates. The latter consists of micro aneurysms and hemorrhages. [18, 19].

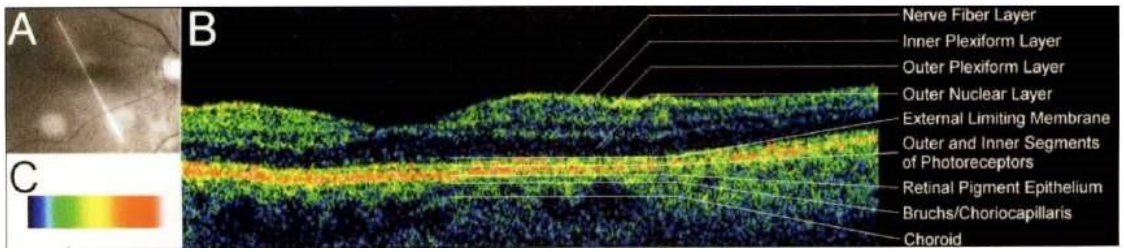

Figure 2.5: An OCT scan of a normal human macula; (a) A frame captured at the start of the scan assists in location, (b) An OCT of the specified scan location, (c) Color map representing the log function of the reflectivity encountered by the probe beam [4].

2.3.1 Soft Exudates or Cotton Wool Spots (CWS)

Soft Exudates or Cotton Wool Spots are acute signs of vascular insufficiency to an area of retina. On retina they appear as white fluffy patches. CWS physically corresponds to swelling in the surface layer of retina. This swelling is the result of ischemia which occurs due to reduced axonal transport within the nerves. The retina shows advance signs of diabetic retinopathy including two pale cotton wool spots as shown in the Figure 2.6(c).

2.3.2 Hard Exudates (HE)

Hard Exudates are lipoprotein and other kinds of protein that originates from micro aneurysms. HE appears as small white or yellowish white deposits with sharp margins. They have irregular shape and variable size as shown in Figure 2.6(b). The coordinates of these lesions are deeper in the retina than cotton wool spots.

2.3.3 Drusen

Drusen are yellow deposits under the retina and made up of lipids (fatty protein) called Bruch's membrane. They shows a sign of dry age-related macular degeneration. Drusen usually may not affect vision but patient may lose peripheral (side) vision. Figure 2.6 (f) shows an example of patient suffering from drusen.

2.3.4 Micro Aneurysms (MAs)

The earliest noticeable indication of retinal image are micro aneurysms. MAs appear on the retinal surface with sharp margins and appear as small, dark and round red dots. These protrusions leak blood into the retinal tissue surrounding it. Most micro aneurysms are reversible with treatment of diabetes, high blood pressure and other disorder causing them. Figure 2.6 (e) shows an example of two MA lesions.

2.3.5 Hemorrhages (HEM)

This type of disorder occur due to leakage of weak capillaries and can result into temporary or permanent loss of visual accuracy. These are categorized in dot, blot and flame shapes. Dot or Blot is commonly associated with diabetes. Flame hemorrhages is a rupture on retinal nerve fiber layer of superficial pre-capillary arterioles, small

veins. HEM are described as red spots with uneven, or distinct edges. Sizes of HEM are greater than MA sizes as shown in Figure 2.6 (b)

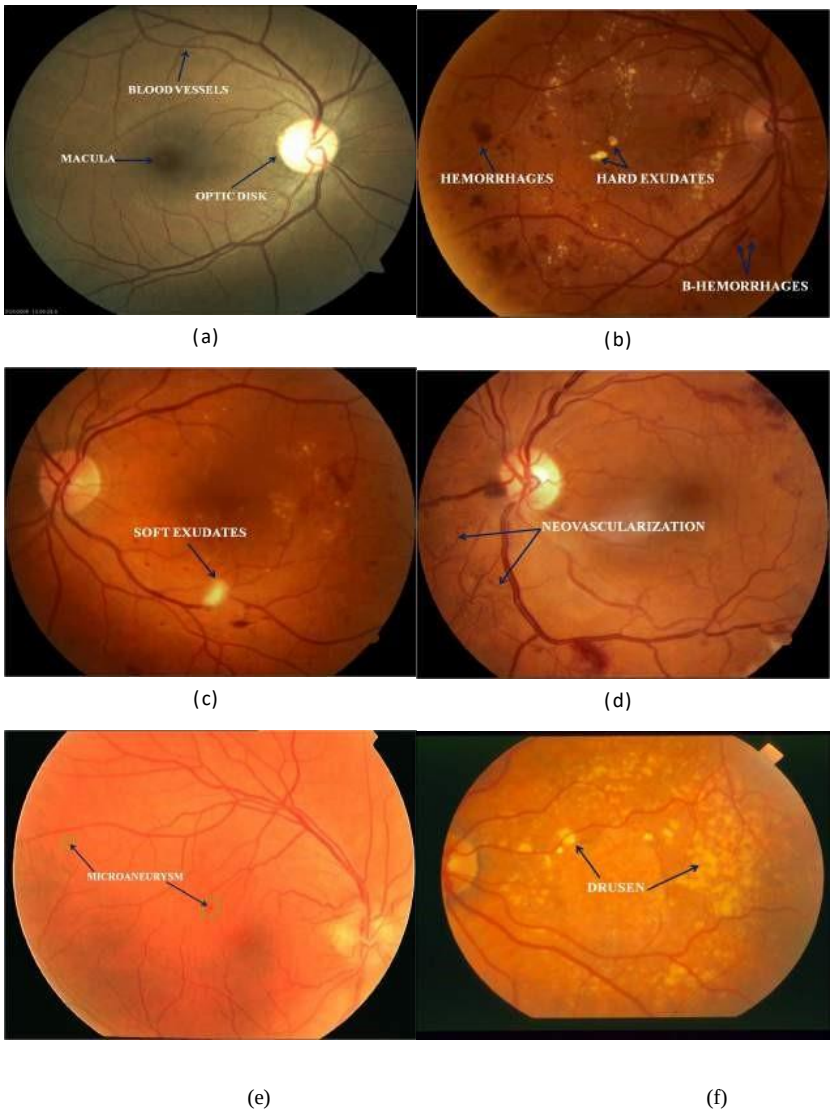

Figure 2.6: Typical fundus images; (a) normal, (b) Hemorrhages, and Hard exudates (c) Soft exudates, (d) Neovascularization, (e) Micro aneurysms, (f) Drusen [5].

2.4 Diabetic Eye Diseases

Diabetes Mellitus (DM), commonly referred as diabetes is a chronic, lifelong condition that affects one's body ability to capitalize the energy found in food. This condition occurs when either the pancreas can't produce enough insulin or the cells in your body have become resistant to insulin. Diabetes can cause long term systematic complications that affect heart, nerves, blood vessels, kidneys and eyes [5]. If diabetes

left untreated, a patient might suffer from serious health problems. An estimated 415 million people had diabetes worldwide, as of 2015. The global economic cost of diabetes was estimated to be US$612 for the year 2014. In Unites States, an individual between 18 and 70 years of age are the most common sufferers with diabetes.

2.5 Diabetic Retinopathy (DR)

Diabetic Retinopathy usually affects the people who had diabetes for significant number of years. DR is a micro vascular complication that damages blood vessels supplying the retina. If not properly diagnosed on time it could result in vision loss [7]. Retina of both the eyes get damaged but all these can be prevented if early treatment is done. Two different scenes viewed by a normal person and a person suffering from diabetic retinopathy is shown in the Figure 2.7 (a) and (b). Classification of DR is done in four stages [8].

Figure 2.7: Normal vision and the same scene viewed by a person with diabetic retinopathy; (a) Normal vision, (b) Scene viewed by a person with diabetic retinopathy [6].

2.5.1 Mild Non Proliferative Retinopathy

The elements of gentle/mild non proliferative retinopathy are a portion of the most punctual indications of diabetic retinopathy. Now, micro aneurysms happen alongside hemorrhages and cotton fleece spots. It merits pointing out that not all patients will see an adjustment in their vision.

2.5.2 Moderate Non Proliferative Retinopathy

Numerous more micro aneurysms, hemorrhages, and cotton fleece spots start to show up, notwithstanding further harm to retinal veins. In this way, the blood stream to the encompassing retinal tissue is lessened giving ascend to vision misfortune.

2.5.3 Severe Non Proliferative Retinopathy

At this stage, blood flow is denied to the expansive ranges of the retina. Accordingly, these zones of the retina send signs to the body keeping in mind the end goal to deliver fresh recruit vessels to improve sustainance.

2.5.4 Proliferative Retinopathy

Proliferative retinopathy is the more propelled type of diabetic retinopathy. At this stage of the disease, fresh vessels begin to develop as the retina sends signs to the body for sustainance improvement. These fresh vessels are unusual and delicate which develop inside and along the different parts of eye and retina respectively. These veins don't characteristic indications or vision misfortune without anyone else's input. Be that as it may, their dividers are thin and delicate, at whatever point they spill blood extreme vision misfortune and even incurable visual impairment can happen.

CHAPTER 3

LITERATURE SURVEY

The developing predominance of diabetes overall expands the quantity of cases that should be surveyed by doctors. Furthermore, the cost involving the regular check ups and examination are very high and absence of expert specialists keep many people away from accepting a sufficient and effective medication. PC helped in discovering CAD frameworks of retinal injuries caused by diabetes, that can allow doctors to have many intriguing advantages both in screening and medical process. In the previous, it will give the chance to analyze huge datasets of retinal images. In the last mentioned, average examination expenses can be lessened as a result of decreasing the workload of prepared classifiers. In writing, a wide assortment of CAD frameworks to identify retinal elements and injuries include three principle steps.

The initial step is the preprocessing keeping in mind the end goal to make up for extraordinary fluctuation between and inside retinal pictures. Green channel is viewed as the most ideal decision, since it gives a greatest difference between various retinal sores and structures. The second step is to remove hopeful sores, in a few approaches include determination method might be performed to remove non-affecting components. The last stride is to order hopeful lesions into ordinary or anomalous. Table 3.1 abridges diverse methodologies used to arrange pictures with splendid injuries, for example, different lesions as far as preprocessing, methodology, classification and results (senstivity, specificity and accuracy are concerned). The important and handy work has been done on automating the process of the detection of the diabetic retinopathy. A lot of work has been done on the segmentation of retinal images to identify the lesions of interest and to eliminate parts with similar physical appereance, as that of lesions, in the human eyes. The detailed review of the same is as follows.

3.1 Review of Comprehensive Surveys on Preprocessing Techniques and Classification Algorithms

As inferable from the procurement procedure, the retinal pictures are all the time of low quality that thwarts further examination. Therefore the preprocessing of these acquired coloured fundus images is indespensible task. The need to remove the inferences for the proper study of these coloured retinal images prompted, Aliaa A.A.Youssif et al. 2007[11] reviewed the state of art techniques available for the preprocessing of such images. The authors furthermore provided the best approaches in a concise manner and also introduced their own comprehensive normalization method for the effective removal of the noises in retinal images. The paper discusses three main approaches for image-preprocessing that are used before studying fundus images, namely, mask generation, illumination equalization and color normalization and the effect of these three on the anatomy of these retinal images. Mask generation (Figure 1) does pixels labelling of the (semi) round coloured retinal image as Region of Interest (ROI), in the whole picture, and the background of the image is excluded (i.e. pixels outside the ROI having a place with the dim encompassing area).

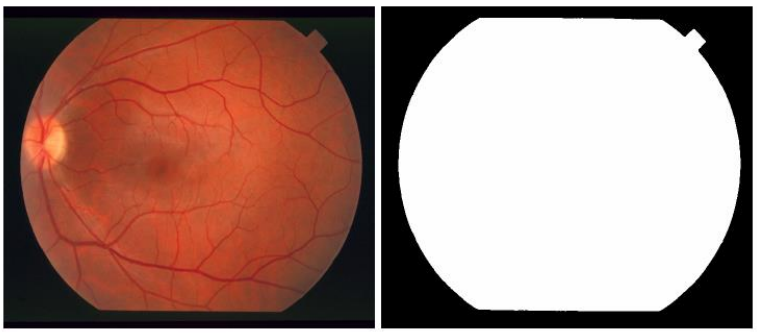

Figure 3.1: Mask generation on retinal image[11].

Further there is a non-uniform illumination in the captured coloured fundus images due to the variety of the retina reaction or the non-consistency of the framework used for collecting the images (e.g. fluctuating the eye position in respect to the camera).The different ways to apply illumination equilization are reviwed. At last the information provided by the color data is conceivably helpful, considering the fact that the color(shading) computation of lesions in retinal pictures demonstrated noteworthy contrasts [11]. With a specific end goal to reliably call attention to shaded items and lesions, colouring must specifically point to the characteristic properties of the images

in question and be self-relaint of imaging conditions. Generally, the conventional methods such as gray scale normalization and histogram equalization are followed to deal with such illumination problems. This is where the authors proposed a comprehensive colour normalization method to get a homogeneous illumination throughout. The author tested their method on the publically available STARE dataset.

The Figures 3.1 and 3.2 demonstrate the effect of mask generation and comprehensive colour normalization.

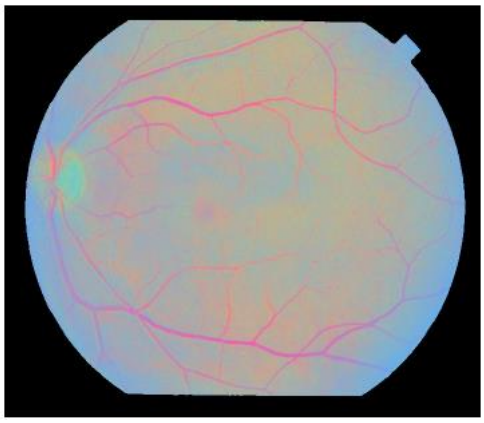

Figure 3.2: Comprehensive normalization of retinal image [32].

Oliver Faust et al. [35] with their paper analysed the algorithms which robotize the extraction of important components that lead to diabetic retinopathy from advanced eye fundus pictures. Besides, various frameworks were examined that utilize these components to person fundus pictures. The groupings extend from straightforward infection no-illness issues to modern sickness seriousness discovery frameworks.

Information regarding the colours was utilized on Bayesian measurable classifier to characterize every pixel into sore or non-injury classes. The method accomplished 100% exactness in identifying all the abnormal retinal pictures having bright lesions (exudates), and 70% ordinary retinal pictures were identified correctly.

A neural network with multiple layers of perceptron's and image processing techniques were combined together to automatically identify the DR and normal retinal pictures respectively. The framework resulted in sensitivity and specificity of 80.21% and 70.66% respectively.

CAD frameworks were used for the discovery of the Non Proliferative Diabetic Retinopathy (NPDR) taking into account the three basic lesions that occur in the human eye if a diabetic person, in particular, hemorrhages and microaneurysms, hard exudates,

and cotton-fleece spots were studied [17].The method could distinguish the NPDR accurately with an exactness of 81.7%.

An effective methodology to identify, ordinary, mellow, direct DR, serious DR and productive DR stages, was studied. The method creates a feature set by using the edges and circumference of RGB segments of the blood vessels in the coloured retinal images. The feature set thus created was fed into a forward feeding ANN. Such an approach achieved accuracy of 85%.

Another approach concentrated on using the the bispectral invariant features as the feed into SVM. The approach was proposed to identify different stages of the DR. The method achieved an accuracy of 93%. The sensitivity and specificity were reported as 90% and 100% respectively.

Thus, the review paper studied the most effective and useful methods proposed so far to classify the abnormal and normal coloured retinal images. The study threw light on the different classifiers and the different features fed to train these classifiers.

3.2 Recent Developments In Automatic Detection Of Diabetic Retinopathy

A lot of researchers are continuously working on proposing automated methods for the detection of DR, Glaucoma and ARMD and different stages involved with such diseases. The studies have been made taking into account almost all kinds of lesions that occur in the human eyes due to diabetes mellitus. Some of recent developments for the same are reviewed briefly as follows:

Nayak et al. [12] considered exudate area regions and the range of veins together with surface elements. The authors extracted all such features in both testing and training datasets. These were fed into the neural system for the classification of images into three classes namely, ordinary, non-proliferative retinopathy and proliferative retinopathy. The recognition were approved by contrasting and evaluating from master ophthalmologists. They exhibited a characterization exactness of 93%, sensitivity and specificity of 90% and 100% respectively. It was implemented on a dataset of 140 pictures.

Clara I. Sánchez et al. [13] focused on the fact that hard exudates are the only early symptoms of diabetic retinopathy. They implemented a five step methodology to

correctly identify the hard exudates from coloured retinal images. The preprocessing was the first step to remove the unwanted interference. The green channel of an RGB image is extracted first. Image enhancement is done by normalizing the luminosity and colours. Next a mixture model based on the probabilistic approach is used in order to disparate the exudates from the background. Finally, edge detection algorithm is implemented to differentiate the hard exudates from the other bright lesions. The method was implemented on the dataset of 80 images. It achieved the sensitivity and specificity of 100% and 90%.

Sidra Rashid et al. [9] extracted the exudates from the retinal images by eliminating the optic disc. The preprocessing involved the technique of histogram equalization. The authors used contrast limited adaptive histogram equalization method for better images. The entropy, standard deviation of the pixels values and the hue are used as the basis for the classification of the images. Fuzzy C-means clustering is done for detecting the regions containing the exudates. The authors have calculated the identification exactness with correlation of master ophthalmologists' hand-drawn ground-certainties and the outcomes are similarly broken down.

Ibrahim Sadek [1] followed an innovative approach to classify the DR and ARMD in the coloured retinal images. The images were preprocessed to conventional intensity normalization. The research is done to examine the bag of words approach. The features are extracted from images using HOG and SURF techniques. The codebook is then generated by using K-means clustering algorithm. The features are pooled to generate single based and multiple based dictionaries. The final classification is done by using SVM’s. The author validated the method on 5 publically available datasets. This resulted in mean accuracies of 97.22% and 99.77% for single and multiple based dictionary approaches.

Harry Pratta et al. [15] recently approached the problem of detecting the diabetic retinopathy by applying deep learning over a relatively very large dataset of the retinal images. The authors built up a system with CNN construction and information enlargement which can recognize the complex highlights included in the arrangement assignment, for example, miniaturized scale aneurysms, exudates and hemorrhages on the retina and thus give a conclusion naturally and without input of user. Before feeding the images into CNN architecture the images were resized and preprocessed. The method achieved an accuracy of 75% on a dataset of 5000 validation images.

Table 3.1: Literature review in tabular format.

Authors	Lesions	Pre-processing	Methodology {State}	Classification {L}	Results SEN %	SPE%	AC%
Ibrahim Sadek [1]	Exudates and drusen	Intensity Normalization	Feature extraction and Bag Of Words(BOW)	SVM's	N/A	N/A	97.22% 99.7%
Sohini Roychowdhury et al. [16]	Exudates and Cotton Wool Spots	MIn MAs Algorithm	Feature Extraction and Ranking	GMM and KNN	100%	53.16 %	90.74%
Clara I.Sánchez et al. [13]	Hard Exudates	Intensity Thresholdin	Edge Based Detection	MIxture Models	90.2 %	90%	N/A
Harry Pratta et al. [15]	Exudates, Drusen and Microaneurysms	Colour Normalization	N/A	CNN	95.5 %	N/A	75%
Daniel Welfera et al. [20]	Exudates	CLAHE	Mathematical Morphology	N/A	70.48 %	98.84 %	N/A
Huan Wang et al. [10]	Exudates	Brightness Adjustment	Local window based verification	Statistical Classification	N/A	N/A	70%
Nayomi Geethanjali Ranamuka et al. [21]	Exudates	Morphological Image Preprocessing	Elimination of Optic disc	Adaptive Fuzzy Algorithm	75.43 %	99.99 %	N/A
Sidra Rashid et al. [9]	Exudates	BPDFHE And CLAHE	Edge Detection And Threshold	Fuzzy C-Means	78.45 %	90.45 %	N/A
T.Walter et al. [22]	Exudates	Grey Scale	Morphological reconstruction	N/A	92.80 %	N/A	92.4%

Authors	Lesions	Pre-processing	Methodology {State}	Classification {L}	Results SEN %	SPE%	AC%
Nayak et al. [12]	Exudates and Blood Vessels	Color Normalization	Feature Extraction	Neural Network	90%	100%	93%

CHAPTER 4

METHODOLOGY

We propose a method for the automatic identification of the bright lesions in retina that is the major cause of diabetic retinopathy. The identification of the exudates (bright lesions) is done by following state of art pre-processing techniques. Firstly, the grey scale conversion of the image is done and green channel of an RGB retinal images is extracted, respectively. The comparison between the two images (grey scale image and green channel image) is done. Green channel image is chosen as the basis image for subsequent steps as this channel provides the best contrast between the bright spots and the background of the image. A median filter is applied to remove the background illumination. Contrast local adaptive histogram equalization is applied to improve the image quality. Then closing morphological methods are followed using a disk of size 6 to dilate and erode the holes and gaps. Then the images is subjected to binary thresholding to highlight the bright lesions only. The feature extraction is carried out using the HOG technique. The final feature set is divided into the testing and training data. The classifier models such as SVM, ANN and random forest are trained using the training dataset. The models are validated using the testing data. The classification of the coloured retinal images is done for the normal and abnormal retinal condition. Finally the ensemble of these models is done to achieve higher accuracy.

This chapter explains in detail the methodology followed to identify the exudates and classify images for the DR. The subsequent sections explain the steps followed in right order as follows: Section 4.1 discusses the different steps of pre-processing techniques and their fundamentals in brief. Section 4.2 explains the morphological methods involved for the erosion and dilation of the pre-processed image. Section 4.3 describes the feature extraction from digital coloured images and the techniques implemented to achieve the same during this work. Last section, Section 4.4 focuses on the different classifiers and the ensemble model of those classifiers that are used for the classification of abnormal and normal retinal images based on the presence of the exudates. The flowchart in Figure 4.1, lays out the steps in a simple and self-explanatory way.

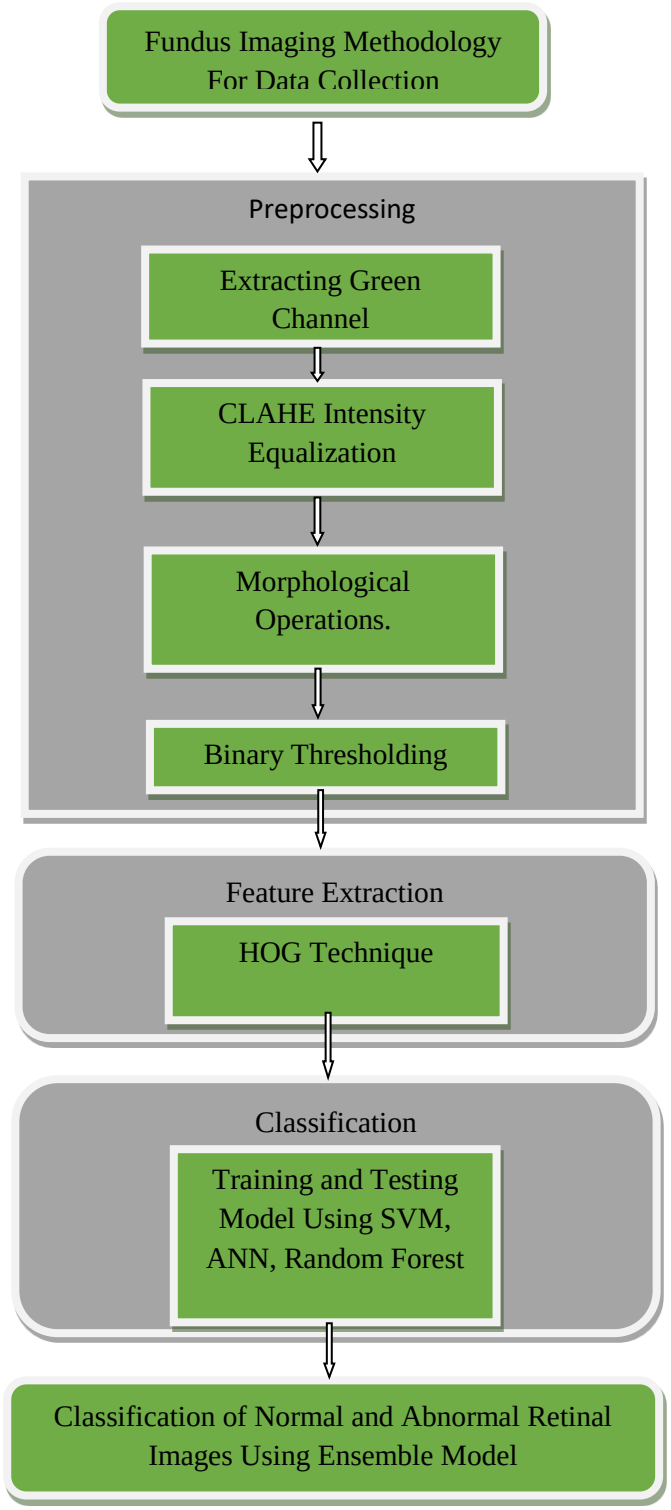

Figure 4.1: The flowchart for the methodology followed.

4.1 Image Pre-processing:

The retinal images acquired by using the fundus camera at first step pre-processed. The goal of pre-processing is to normalize the different variation in the image. The illumination, contrast and colour are the most important factors that vary in the image [22]. The variation among these factors may also result in unwanted noise that creates hindrance in effectively studying the images. The variations can be within the images or between the images within the dataset. There are some external causes for such unwanted variations between the images like different cameras used to capture the images, varied illumination at the time of capturing, angle used for image acquisition, and difference in the pigmentation of eyes of two individuals [27]. Thus to deal with all such nuances in coloured retinal images different techniques are tried to achieve these goals. The same are mentioned below.

4.1.1 Grey Scale Conversion

The images in digital image processing comprise of mainly three basic colours namely red, green, and blue, thus are often called RGB images. Each pixel in an RGB image contains three values (between 0-255) for each of the three colours respectively. The combination of these three values gives a particular colour to that pixel in an image. The process of converting the RGB image to a grey scale image helps to make the image more uniform. The grey scale image uses all the three values of red, green and blue by taking into account only a factor of these three channel values as follows:

$$I = 0.299*R + 0.587*G + 0.114*B;$$

Where I is the resulting grey scale image, R is the pixel colour value of red channel, G is the pixel colour value of green channel and B is the pixel colour value of blue channel.

The major reason to convert the images to grey scale is to reduce the complexities that occur due to colour. The inherent complexity of the grey scale image is much less as compared to a RGB image. The advantage being that the terms like contrast, textures, edges, shape, etc. can still be studied without the colour component involved.

4.1.2 Green Channel Extraction

As it is already stated that an image has three separate channels. All three can be extracted separately but the red channel has over saturation of red colour while blue channel is noisy and under saturated thus not feasible. So, green channel is chosen. The Figure 4.2 below shows that the difference in contrast between the grey scale image and the green channel of an RGB image.

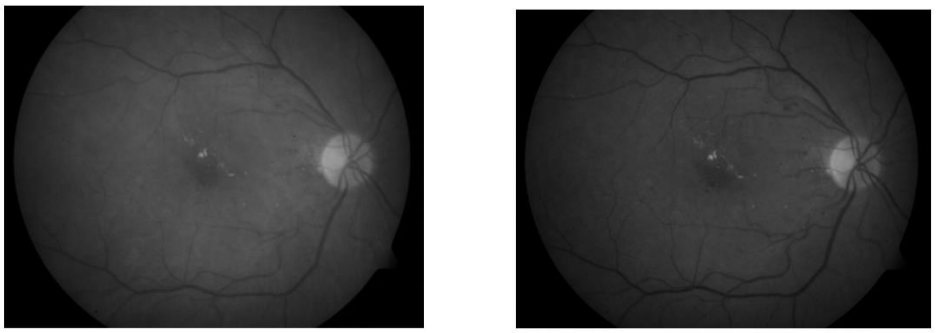

(a) (b)

Figure 4.2: (a) Grey scale image (b) Green channel of the image.

As it can be observed from the figure 4.2 that the contrast between the bright spots and the background is much more subtle in the Figure 4.2 (b) image i.e. the green channel of image. Thus in this study green channel image is chosen as base for further pre-processing of dataset of retinal images.

4.1.3 Median Filtering:

The green channel thus extracted from the RGB image for the further process is subjected to median filtering. The illumination in the background due to the fundus camera and the optic disc illumination makes it difficult to separate the bright lesion in the centre. Thus median filtering is applied to the image and then this filtered image is subtracted from the original green channel of the image. This results in much better normalized image.

4.1.4 CLAHE

CLAHE stands for contrast limited adaptive histogram equalization. Histogram equalization is well known and commonly used enhancement technique in the digital image processing. This is also known as Adaptive Histogram Equalization (AHE). It works by changing the image in such manner as to have a desired intensity histogram.

It does so by altering the intensity range and contrast of the image. This can be done by using the CDF as mapping function. The CDF can be defined as follows:

$$f_i(i_k) = \frac{n_k}{N};$$

$$F_k(i_k) = \sum_{j=0}^{k} f_i(i_j);$$

Where N is the total number of pixels, n_k is the no. of pixels with intensityi_k.

But if the image under consideration has a very limited intensity range then AHE implementation results in the enhanced noise. The enhancement in the contrast for intensity level at some region is directly proportional to the slope of CDF at that particular intensity level. The slope of CDF is determined by the height of the histogram at that intensity level. Thus we can limit the amount of contrast enhancement by limiting the height of histogram (slope of the CDF) at that particular intensity level. The process of limiting this height is called CLAHE.

4.1.5 Binary Thresholding

It is one of the easiest and simplest method used for segmenting the images. As it is clear by the name it converts any given image into a black and white image. It works on the concept of defining a certain threshold value for intensity. Thus all the pixel having value above that threshold value attain an absolute value of 255 i.e. white, and all the pixels having value below that threshold, goes down to 0 i.e. black. Figure 4.3 gives an example of binary thresholding for the normal retinal image.

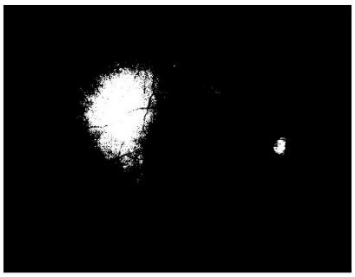

Figure 4.3: Binary thresholding of normal retinal image.

4.2 Opening and Closing Morphological Methods

The image obtained after the binary thresholding has unwanted white patches. It also has some holes and the exudates in the centre are not distinctive enough. The opening

and closing operations are applied to the binary image to remove the unwanted with patches and to have a clearer image. The effect can be seen in the Figure 4.4 below.

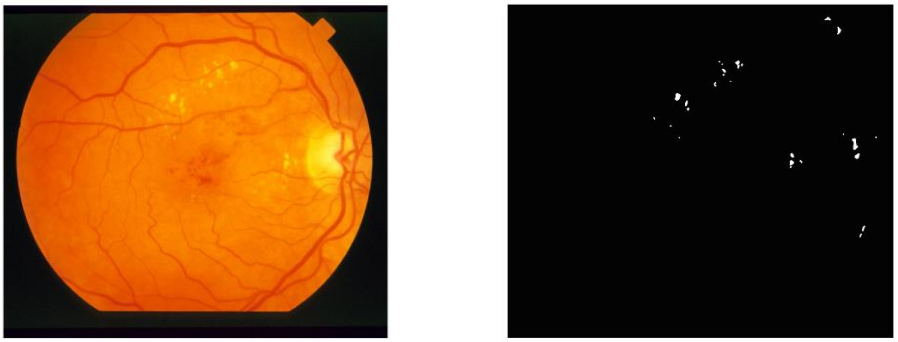

(a) (b)

Figure 4.4: (a) The original retinal image (b) The image after the binary thresholding and morphological operations, exudates are identified.

The morphological opening and closing operations consist of two parts described as follow

1. Erosion: The erosion of a binary image is nothing but removing the unwanted bits of the white foreground that are not useful or are unnecessary for the futher process. It works by first selecting a structuring element. The structuring element is basically a matric with binary values. The example of structuring element with a shape of disk is shown below in Figure 4.5.

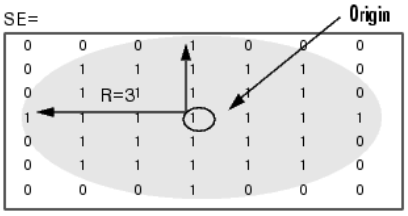

Figure 4.5: The structuring element of disk shape.

Mathematically the erosion of the binary image I by structuring element S can be defined as:

$$I \ominus S = \{z \in E | S_z \subseteq I\};$$

Where E is the grid of integers, I is an binary image, and B_z is the form of B translated by z. Here the operation can be defined as follows.

$$S_z = \{s + z | s \in S\}, for\ all\ z \in E.$$

At the point when the structuring component S has a middle (e.g., S is a disc or a square), and is situated on the centre point of E, at that point the disintegration of A by B can be comprehended as the locus of pixels that can be reached by the focal point of B when S moves inside I. For instance, the disintegration of a square of side 10, focused at the starting point, by a disc of span 2, likewise focused at the birthplace, is a square of side 6 focused at the origin.

The erosion can also be expressed as:

$$I \ominus S = \bigcap_{s \in S} I_{-s}.$$

2. Dilation: The dilation is opposite of the erosion and it can be defined as:

$$I \oplus S = \bigcap_{s \in S} I_s$$

The dilation is also commutative that means, $I \oplus S = S \oplus I = \bigcup_{i \in I} S_{i.}$

To explain in words the above equations mean that if the centre of the structuring element is at the origin then dilation of image I by S can be understood as the locus of the pixels of image that can be overlapped by S when S slides inside I. Using the same example as above, for the dilation of the square of side 10 by a disk with radius 2, will be a square of side 14.

The dilation can also be obtained by:

$A \oplus B = \{z \in E | (S^{sy})_z \cap A \neq \emptyset\}$, where S^{sy} denotes the symmetery of S, such that, $S^{sy} = \{x \in E | -x \in S\}$.

Thus dilation can be used to thicken the very thin and lightly drawn images.

The opening operation is the combination of eroding the image first so as to make the unwanted elements thin and and then apply dilation to thicken the elements which are still there after erosion. This clarifies the elements which are to be focused upon. The espression i.e. given below;

$$I.S = (I \ominus S) \oplus S$$

where I is binary image and S is structuring element.

The closing operation is exactly opposite of the opening operation. It proceeds by dilating the image first then eroding the grainy non useful elements. The expression for the closing can be shown as follows.

$$I.S = (I \oplus S) \ominus S.$$

4.3 Feature Extraction

Features assume a critical part in the zone of image handling. Before moving on to get the features from an image, different pre-processing methods like binarization, thresholding, resizing and so on are implemented on the image under consideration. From that point onward, extraction strategies are followed to get features that will be helpful in arranging and acknowledgment of various images. Extraction of features are important in different image preparing applications e.g. recognition of characters. As features characterize the image behaviour, they demonstrate its size as far as memory space is considered, effectiveness in grouping/clustering furthermore, clearly in saving time too.

Choosing the most significant features is an essential venture during the time spent in classification issues particularly in penmanship recognizable proof since: (1) it is vital to locate all existing subsets of features that can be shaped from the underlying set which result in waste of time, (2) each feature is significant at any rate of discrimination, and (3) variance inside intra-class and between the classes is not all that much high. Past a certain point, the consideration of extra elements leads to a worse instead of better execution.

There are many algorithms available for the extraction of meaningful features from the coloured images. After spending a good time on studying these various techniques like local binary pattern, speeded up robust features, scale invariant feature transform, hough transform etc., it was observed that though SURF and LBP work fine with the fundus images for the classification of diabetic retinopathy, HOG (Histogram of Gradients) is the most effective technique in this case because of its lower dimensionality and more discriminating power.

The descriptors in HOG are acquired as like [36] (Section 4.3.1). Each channel of image is separated into settled number of squares with a size of 32 ×32 pixels, at that point each piece is subdivided into 4 cells (with a size of 16 × 16 pixels), thus each piece adds a measurement of 31 to the component histogram. For each channel, the

histograms are linked vertically framing an element lattice of a size 31 × number of pieces. Altogether, the three channels will constitute an element lattice of a size 93 × number of pieces. The invalid descriptors beginning from the dark region encompassing the fundus picture are not considered. Figure 4.6 demonstrates an illustration of extraction of HOG descriptors.

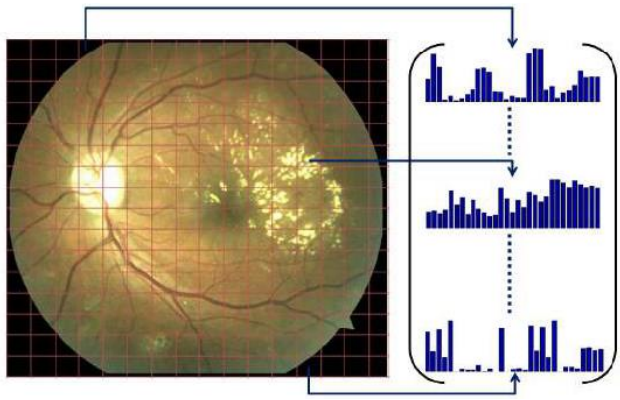

Figure 4.6: HOG descriptors [36].

4.3.1 Feature Extraction Using HOG:

The Histogram of Oriented Gradients (HOG) presented by Dalal et al. [36] are descriptors of image features utilized in PC vision and digital image processing (DIP) for identification of objects. The general procedure can be abridged as examined underneath.

The descriptors in HOG features are represented by the distribution of the direction of the gradients. The oriented gradients are calculated for each pixel and arranged in the bins or histograms. Slopes/gradients (derivative of x and y) of an image are extremely helpful on the grounds that the size of slopes is expansive around edges and corners (areas of rapid change in intensity) and we realize that edges and corners pack in significantly more data about image in question shape than regions of constant intensity and colour.

The HOG descriptors are calculated by first finding the horizontal that is x axis and vertical that is y axis slopes/gradients. This can be easily achieved by using [-1, 0, 1] kernel and its transpose. By filtering the image with such a kernel in both directions it is possible to achieve the maximum change in the pixel value with its direction. This value is called oriented gradient. The resulting image will have x-gradients shooting up

in the vertical directions and y-gradients shooting up in horizontal directions. It can be easily observed that these values of oriented gradients are large around edges. The image will have sharp colours around the edges and will be flat along the constant colour and intensity regions. As there are three channel values (RGB) for a pixel the maximum value of gradient along all three channels is assigned to that particular pixel and the angle of this maximum gradient is chosen as the orientation. A general example of such effect can be shown in figure 4.7 below.

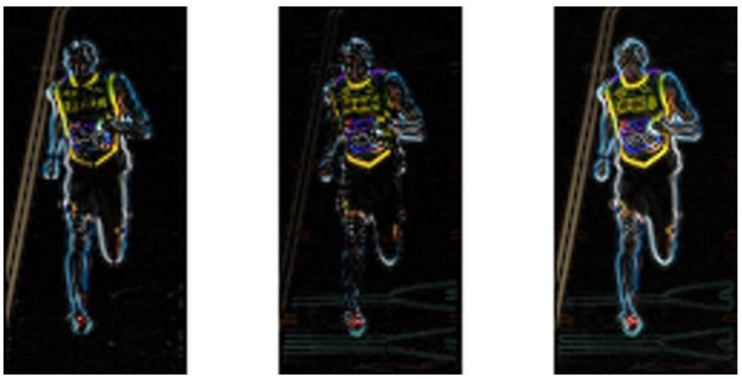

(a) (b) (c)

Figure 4.7: (a) Absolute value of x gradient (b) Absolute value of y gradient (c) Absolute value of the both gradients[36].

Also the absolute value of and the orientation can be calculated by the following simple equations:

$$g = \sqrt{g_x^2 + g_y^2};$$

$$\emptyset = arctan\frac{g_y}{g_x};$$

where g is the absolute gradient, g_x is the gradient in the x direction, g_y is the gradient in the y direction, $\emptyset$ is the orientation of the g. All the values are for a particular pixel.

The image is divided into the patches of selected size say 8*8. Thus the values of gradients are calculated for the each pixel in these patches. Each pixel in the patch has two values; the gradient and orientation. This gives a total of 8*8*2 = 128 values in the patch of the image, if a patch size of 8*8 is chosen. These value are then distributed in the 9 bins. Each bin correspond to an orientation value starting from 0 and going up to 160, i.e. 0,20,40,80,10,120,140 and 160 respectively. The values are distributed among these bins depending upon the orientation values. Thus making a 9*1 vector for such a

patch. This vector can also be called histogram of oriented gradients. The distribution can be understood in figure 4.8.

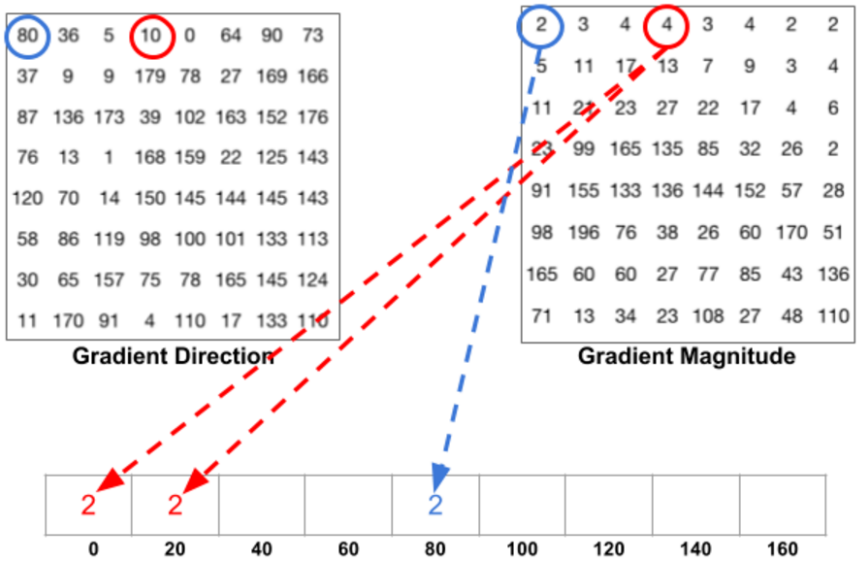

Figure 4.8: The distribution of gradients in the bins [36].

Next we normalize the histogram by using a bigger say 16*16 window. If such a window is chosen then it contains four windows of 8*8. Thus the histogram are concatenated vertically and a 36*1 vector is obtained. This vector is normalized to make it independent of lighting and colour variations. Such process is repeated for all possible windows of selected size over the image. The final descriptors are calculated by horizontally concatenating the results for all these 16*16 patches of windows. An example of the histogram of oriented gradients can be seen in figure 4.9.

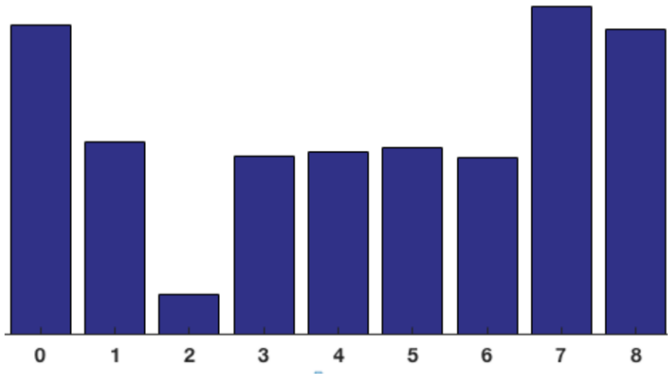

Figure 4.9: Histograms of the oriented gradients [36].

Thus it can be seen that the HOG feature extraction is robust and discriminative technique to achieve the most useful and important features that define the image.

4.4 Classification and Ensemble

The HOG features extracted are collected in a feature table for all of the dataset. The classification of the images for the non-proliferative diabetic retinopathy based on the presence of the exudates in the retinal images is done by the classifiers such as Random Forest, KNN and SVM. The brief description of the three classifiers is given in the subsequent sections.

4.4.1 Random Forest

This is an ensemble learning technique for regression, classification and other machine learning tasks that works by analysing the various features at the training time. Features analysis is much important as a result their priority is decided and according to these priority multitudes of decision tree is constructed. Output of this tree is mode of the class (for classification type problem) or mean prediction of individual tree in the case of regression problems. Each tree in random forest has capability to influence the whole decision since each tree is designed on the basis of importance of features and finally results of all tree is aggregated to find out the target result.

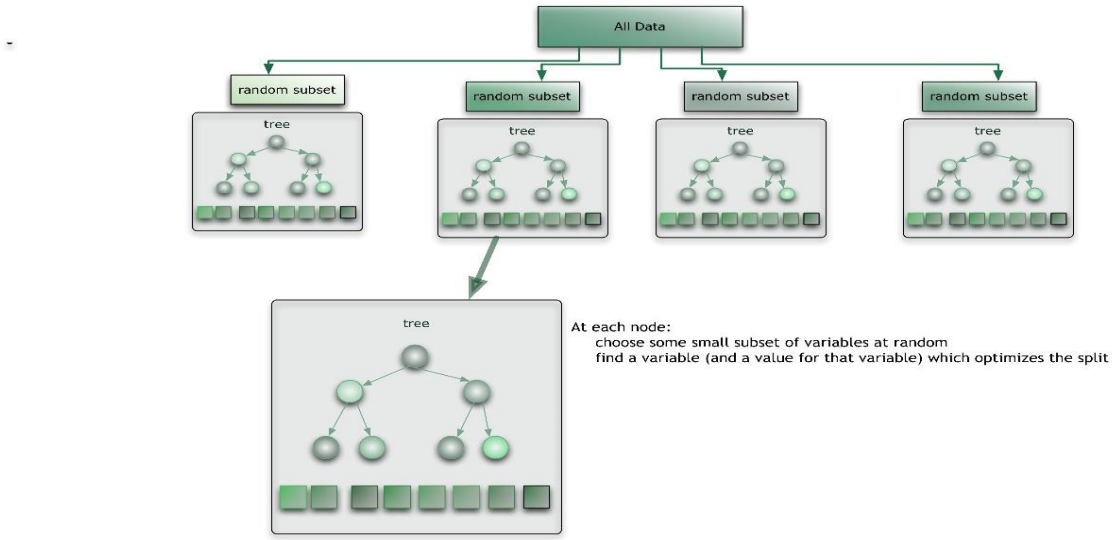

Figure 4.10: Random forest working illustration [36].

4.4.2 Support Vector Machine

SVM is a supervised machine learning approach used for both type of problems classification as well as regression. But most of the time it is used to solve classification problems. In this technique we plot the all features as a data point in dimensional space by using coordinate values. Then we create a hyperplane that can discriminate the two classes easily.

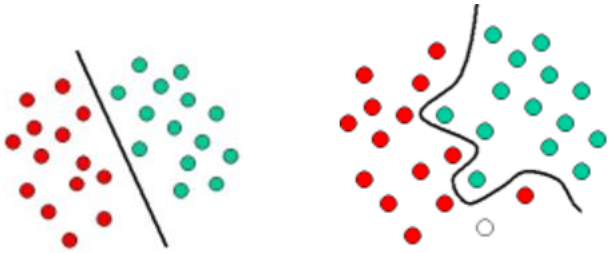

(a) (b)

Figure 4.11: (a) Linear SVM (b) Nonlinear SVM[37].

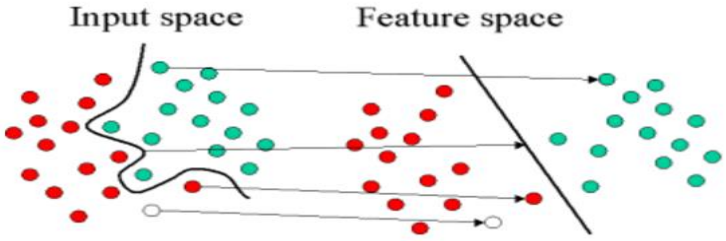

Figure 4.12: Mapping to rearrange the values and find optimal line [37].

Every line present in above figure which is separating our training data couldn't be the best solution so the only line that can act as hyperplane can be selected as the solution which maximizes the margin of training corpus or data like below figure 4.13.

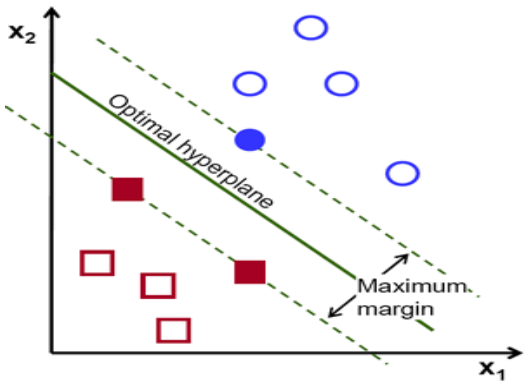

Figure 4.13: Support vector machine hyperplane maximizing margin [37].

4.4.3 Multi Layer Perceptron

The multi layer perceptron is nothing but artificial neural network. To be specific it is a type of feedforward neural network. It comprises of a minimum of three layers of perceptrons. The nodes/perceptrons use non-linear activation function. It uses the backpropogation algorithm for robust training. The very use of backpropagation and multiple layers distinguish MLP from the normal feed forward linear propagation.

As described above the non linear activation function. It commonly uses two activation functions, both are sigmoid in nature and can be described as below.

$$y(v_i) = \tanh(v_i)$$

$$y(v_i) = (1 + e^{v_i})^{-1}.$$

where $y_{is}$is the output from the i^{th} node and v_i is the weight associated with the corrections made in input. The first fucntion is hyperbolic tangent while the second function is logistics function. Also the function that adjusts the weights and make corrcetions, minimizes the following function.

$$\varepsilon(n) = \frac{1}{2}\sum_j e_j^2\,(n)$$

where ε is the total error in the model, $e_j$is the error in the j^{th} node.

The figure below explains and clarifies the MLP process for classification.

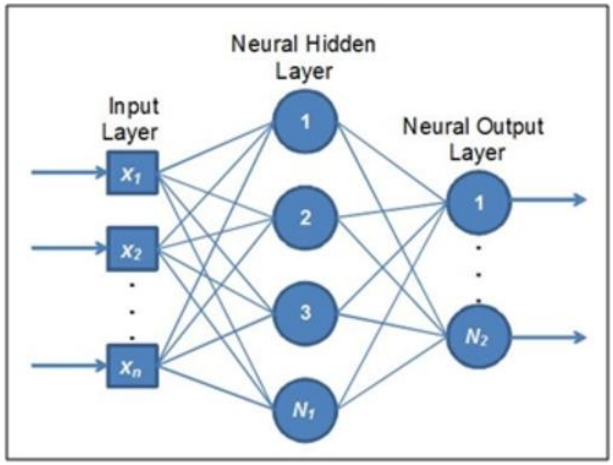

Figure 4.14: The basic layers of MLP [38].

4.4.4 KNN

K-Nearest Neighbor is a non-parametric managed learning method utilized for classification work. The guideline behind closest neighbor strategies is to discover a predefined number of preparing tests nearest in separation to the new point and foresee the name from these. The quantity of tests can be a user characterized steady or change in view of the nearby density of points. Standard Euclidean distance is the most widely

recognized decision for metric measure. The figure below will make the working of the KNN clear.

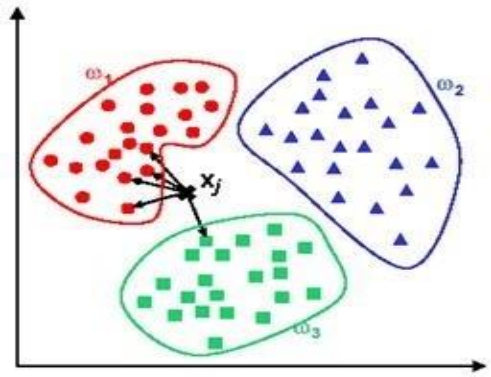

Figure 4.15: KNN assigns class to an object by checking its distance [38].

The figure above is self-explanatory the clusters of different classes are formed. Each new object is assigned to a particular class by calculating its eculidean distance from the centre of each cluster. The cluster having a minimum distance from the object is assigned to it.

4.4.5 Ensemble of Models

Ensembling is a strategy in which we manufacture numerous models in view of comparable or unique methods and later join them, keeping in mind the end goal to achieve high accuracy. The thought is to make a stronger prescient model which retains forecasts from various systems. In layman terms, it is thinking about supposition from all pertinent individuals and later applying voting framework or giving equivalent or higher weightage to a few people.

The error that emerges when we stick to the single model for the classification is the reason to use the concept of ensembling. To understand this, the different components of error are to be understood first. The equation [39] below explains the error in any model.

$$Err(x) = (E\left[\hat{f}(x)\right] - f(x))^2 + E(\hat{f}\ (x) - E\left[\hat{f}(x)\right])^2 + \ \sigma_e^2;$$

$$Err(x) = Bias^2 + Variance + Irreducible\ Error;$$

The terms bias and variance are defined below:

Bias error: This terms helps to judge how far are the, values predicted by our model, from the actual model. A high bias is the proof that our model is not performing well and is missing the underlying relations or trends.

Variance error: The variance term defines how far are the, values predicted by our model from each other. Here the variation with in the predicted values is studied. Any model with high variance will not perform well on the unseen or testing data.

The figure 4.15 describes the two error.

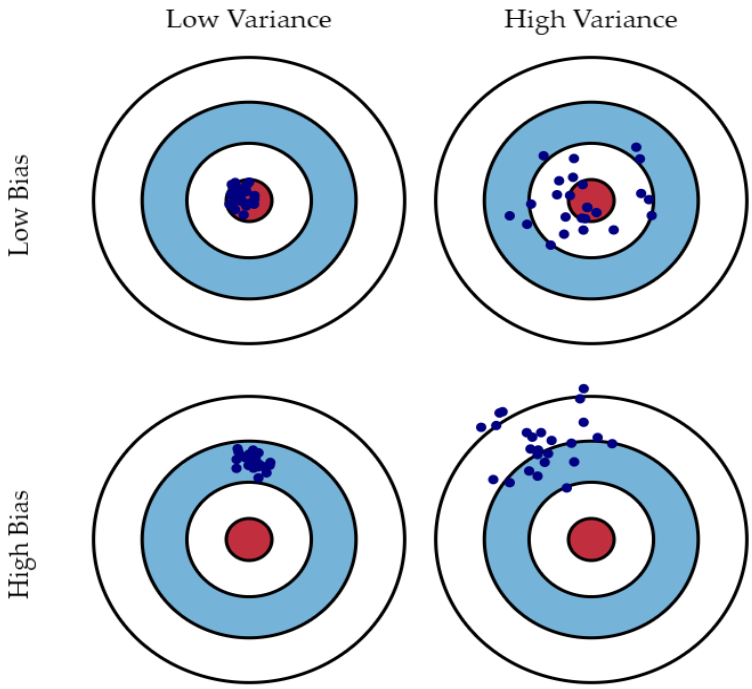

Figure 4.16: The graphical representation of bias and variance [39].

As the complexity of the model increases the error term of the model reduces upto a certain threshold due to the reduction in bias. But after a certain point the error starts to increase again at a rapid rate as higher complexity leads to higher variance. Thus a balance should be maintained between these two errors for having a robust model/classifier. The concept of ensembling two or more models helps us to achieve this balance between bias and variance [39].

There are a lot of techniques that are helpful in successfully ensembling the models and achieve better results than running individual models. Techniques like bagging, boosting, stacking, weighted average etc. are some ways to ensemble the two or more models. The ensembling in this research is done to explore all possible combination

methods. There are nine combination methods used to combine SVM, MLP and KNN models. The methods that gave best results are listed below.

1. **Majority Voting**

   Every model makes a prediction (votes) for each test instance and the final output prediction is the one that receives more than half of the votes. Although this is a widely used technique, one may try the most voted prediction (even if that is less than half of the votes) as the final prediction. This method is sometimes called "plurality voting". The mathematical expression for the same can be expressed as below

$$\sum_{t=1}^{T} C_{t,k} = max_{j=1}^{e} \sum_{t=1}^{T} C_{t,j}$$

   where d_j is the decision made by D_t classifier.

2. **Bayes Optimal Classifier Learning**

   The Bayes Optimal Classifier is a grouping strategy. It is a gathering of the considerable number of speculations in the theory space. On average, no other outfit can beat it. Each speculation is given a vote relative to the probability that the preparation informational index would be examined from a framework if that theory were valid. To encourage preparing information of limited size, the vote of every theory is likewise duplicated by the earlier likelihood of that speculation. The Bayes Optimal Classifier can be communicated with the accompanying condition:

$$Y = argmax_{x_j \in E} \sum_{h_i \in H} P(x_j|h_i)P(T|h_i)P(h_i)$$

   where, Y is the predicted class, E is the set of all possible classes, H is the hypothesis space, P refers to the probability and T is training data.

3. **Decision Template**

   Decision templates were introduced by Kuncheva in 2001 [44]. It works by combining the continuous valued output of ensemble classifiers. The outputs by the different classifiers are typically normalized to add upto 1. The softmax normalization can be expressed as follows

$$y_j'(x) = \frac{\exp\{y_j(x)\}}{\sum_{k=1}^{c} \exp\{y_k(x)\}}$$

Where $y_j'(x)$ is the j^{th}output of the y_j classifier.

Here the new values for $y'$are used for the classifier ouput. Suppose x$\in R^n$ is a feature vector say V = $\{v_1, v_2, \ldots \ldots v_c\}$ is the vector for class labels. Each classifier D_t in the ensemble provides a 'c' support to x. The output of all the classifiers is organized into a decision profile. Each row and coloumn then represents the support for the j^{th} class by the classifier D_t.

The decision templates are then obtained using the equation below.

$$DT_j = \frac{1}{N_j} \sum_{X_j \in v_j} DP\ (X_j)$$

Where DT is the decision template and N_j is the number of class j instances. Finally a similarity score can be calculated by using Euclidean distance and a total support for the j class can be computed.

4. Dempster-Shafer

Dempster-Shafer Theory (DST) is a numerical hypothesis of confirmation. In a limited discrete space, Dempster-Shafer hypothesis can be deciphered as a speculation of likelihood hypothesis where probabilities are doled out to sets instead of fundamentally unrelated singletons. In conventional likelihood hypothesis, theory is related with just a single conceivable occasion. In DST, confirmation can be related with numerous conceivable occasions, e.g., sets of occasions. Therefore, theory in DST can be important at a higher level of deliberation without resorting to suspicions about the occasions inside the evidential set. Where the confirmation is sufficiently adequate to allow the task of probabilities to single occasions, the Dempster-Shafer display crumples to the conventional probabilistic definition. A standout amongst the most imperative components of Dempster-Shafer hypothesis is that the model is intended to adapt to changing levels of exactness with respect to the data and no further suspicions are expected to speak to the data. It too takes into account the immediate portrayal of instability of framework reactions where an loose info can be described by a set or an interim and the subsequent yield is a set or an interim.

CHAPTER 5

EXPERIMENTAL RESULTS

The proposed methodology is carried out on publically available dataset of coloured retinal images, MESSIDOR [41]. The data set contains around 400 images of the retinas of the patients suffering from diabetes. The images have a large variation in colour and illumination within and between the images. The example images are shown below.

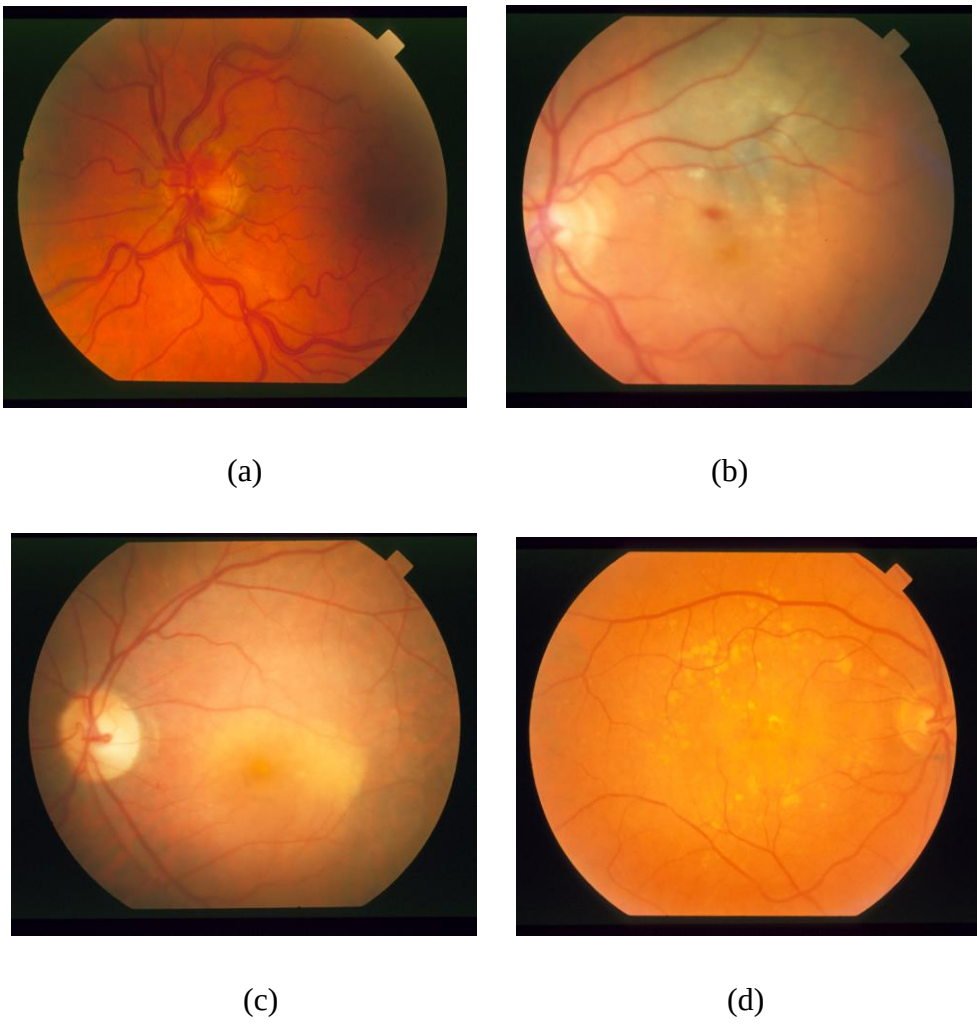

(a) (b)

(c) (d)

Figure 5.1: The images with varying colour and illumination in MESSIDOR dataset (a) Image with red as dominant color, (b) Image having red lesions, (c) An unaffected retinal image, (d) Image of retina with exudates and drusen. .

The efficiency and authenticity is evaluated by using the formulas and defining necessary terms as follows.

$$Accuracy = \frac{Total\ Number\ Of\ Images\ Identified\ Correctly}{Total\ Number\ Of\ Images}\%$$

Or

$$Accuracy = \frac{T_N + T_P}{T_N + F_P + F_N + T_P}\%$$

Where

$T_P(true\ positive)$: DR affected images accurately classified as affected.

$T_N(truenegative)$: Normal images accurately classified as normal.

$F_P(false\ positive)$: Normal images inaccurately classified DR affected.

$F_N(false\ negative)$: DR affected images incorrectly classified as normal.

The value of the false negatives should be kept as low as possible. Efforts have been made in this research to keep the number of F_N as low as possible.

5.1 HOG Feature Table

Images are subjected to the preprocessing and HOG features are extracted on the resized image. The feature table is obtained an shown in figure 5.2.

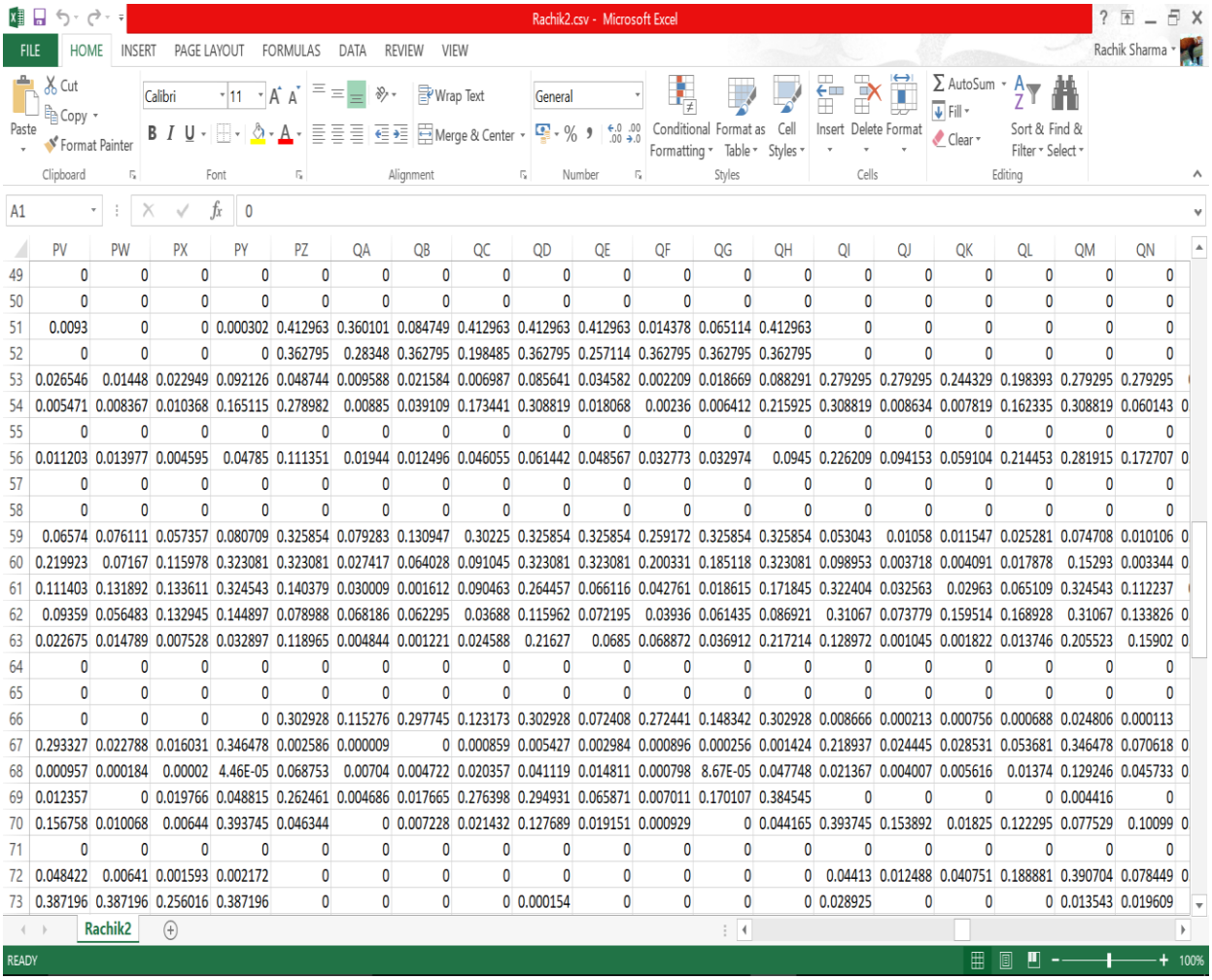

	PV	PW	PX	PY	PZ	QA	QB	QC	QD	QE	QF	QG	QH	QI	QJ	QK	QL	QM	QN
49	0	0	0	0	0	0	0	0	0	0	0	0	0	0	0	0	0	0	0
50	0	0	0	0	0	0	0	0	0	0	0	0	0	0	0	0	0	0	0
51	0.0093	0	0	0.000302	0.412963	0.360101	0.084749	0.412963	0.412963	0.412963	0.014378	0.065114	0.412963	0	0	0	0	0	0
52	0	0	0	0	0.362795	0.28348	0.362795	0.198485	0.362795	0.257114	0.362795	0.362795	0.362795	0	0	0	0	0	0
53	0.026546	0.01448	0.022949	0.092126	0.048744	0.009588	0.021584	0.006987	0.085641	0.034582	0.002209	0.018669	0.088291	0.279295	0.279295	0.244329	0.198393	0.279295	0.279295
54	0.005471	0.008367	0.010368	0.165115	0.278982	0.00885	0.039109	0.173441	0.308819	0.018068	0.00236	0.006412	0.215925	0.308819	0.008634	0.007819	0.162335	0.308819	0.060143
55	0	0	0	0	0	0	0	0	0	0	0	0	0	0	0	0	0	0	0
56	0.011203	0.013977	0.004595	0.04785	0.111351	0.01944	0.012496	0.046055	0.061442	0.048567	0.032773	0.032974	0.0945	0.226209	0.094153	0.059104	0.214453	0.281915	0.172707
57	0	0	0	0	0	0	0	0	0	0	0	0	0	0	0	0	0	0	0
58	0	0	0	0	0	0	0	0	0	0	0	0	0	0	0	0	0	0	0
59	0.06574	0.076111	0.057357	0.080709	0.325854	0.079283	0.130947	0.30225	0.325854	0.325854	0.259172	0.325854	0.325854	0.053043	0.01058	0.011547	0.025281	0.074708	0.010106
60	0.219923	0.07167	0.115978	0.323081	0.323081	0.027417	0.064028	0.091045	0.323081	0.323081	0.200331	0.185118	0.323081	0.098953	0.003718	0.004091	0.017878	0.15293	0.003344
61	0.111403	0.131892	0.133611	0.324543	0.140379	0.030009	0.001612	0.090463	0.264457	0.066116	0.042761	0.018615	0.171845	0.322404	0.032563	0.02963	0.065109	0.324543	0.112237
62	0.09359	0.056483	0.132945	0.144897	0.078988	0.068186	0.062295	0.03688	0.115962	0.072195	0.03936	0.061435	0.086921	0.31067	0.073779	0.159514	0.168928	0.31067	0.133826
63	0.022675	0.014789	0.007528	0.032897	0.118965	0.004844	0.001221	0.024588	0.21627	0.0685	0.068872	0.036912	0.217214	0.128972	0.001045	0.001822	0.013746	0.205523	0.15902
64	0	0	0	0	0	0	0	0	0	0	0	0	0	0	0	0	0	0	0
65	0	0	0	0	0	0	0	0	0	0	0	0	0	0	0	0	0	0	0
66	0	0	0	0	0.302928	0.115276	0.297745	0.123173	0.302928	0.072408	0.272441	0.148342	0.302928	0.008666	0.000213	0.000756	0.000688	0.024806	0.000113
67	0.293327	0.022788	0.016031	0.346478	0.002586	0.000009	0	0.000859	0.005427	0.002984	0.000896	0.000256	0.001424	0.218937	0.024445	0.028531	0.053681	0.346478	0.070618
68	0.000957	0.000184	0.00002	4.46E-05	0.068753	0.00704	0.004722	0.020357	0.041119	0.014811	0.000798	8.67E-05	0.047748	0.021367	0.004007	0.005616	0.01374	0.129246	0.045733
69	0.012357	0	0.019766	0.048815	0.262461	0.004686	0.017665	0.276398	0.294931	0.065871	0.007011	0.170107	0.384545	0	0	0	0	0.004416	0
70	0.156758	0.010068	0.00644	0.393745	0.046344	0	0.007228	0.021432	0.127689	0.019151	0.000929	0	0.044165	0.393745	0.153892	0.01825	0.122295	0.077529	0.10099
71	0	0	0	0	0	0	0	0	0	0	0	0	0	0	0	0	0	0	0
72	0.048422	0.00641	0.001593	0.002172	0	0	0	0	0	0	0	0	0	0.04413	0.012488	0.040751	0.188881	0.390704	0.078449
73	0.387196	0.387196	0.256016	0.387196	0	0	0	0	0.000154	0	0	0	0	0.028925	0	0	0	0.013543	0.019609

Figure 5.2: The feature table after feature extraction using HOG.

As can be seen from the figure above, HOG has extracted the values for the oriented gradients from the images. Each image after resizing to 50*50 pixels provides a vector of 900 features. Thus capturing all the necessary information from an image.

These features are used to train different classifier models namely, SVM, ANN and random forest. The results for these individual models is shown in subsequent sections repectively. The ensenmble of these models is also made at the end to achieve higher frequency.

5.2 Support Vector Machine (SVM)

The results obtained after feeding the feature table with 900 features are displayed below.

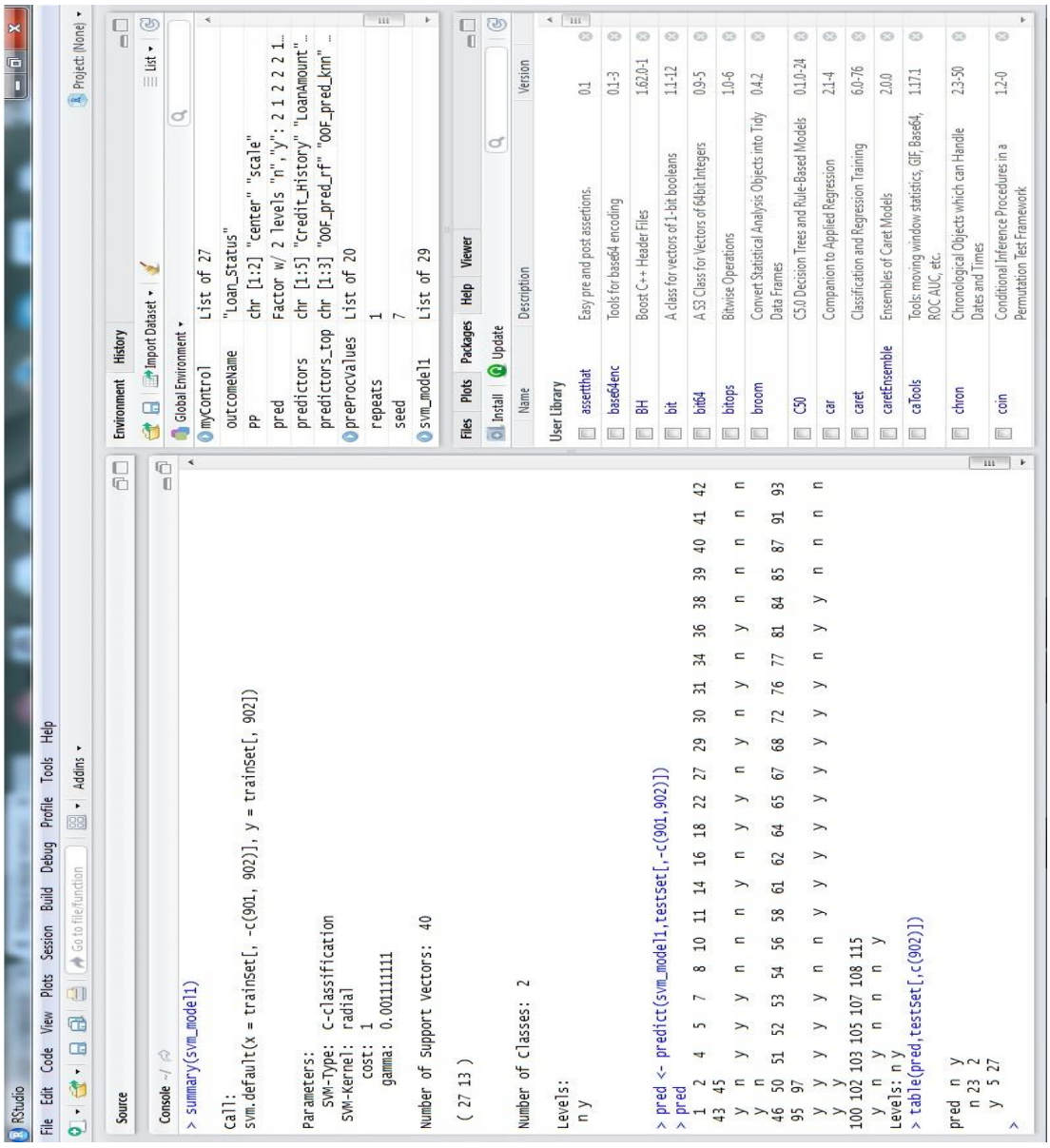

Figure 5.3: Results of SVM

The confusion matrix in the above figure can be used to calculate the accuracy of the model. After feeding the values into the formula of the accuracy specified at the start of this chapter we achieve an accuracy of 88%.

5.3 Random Forest

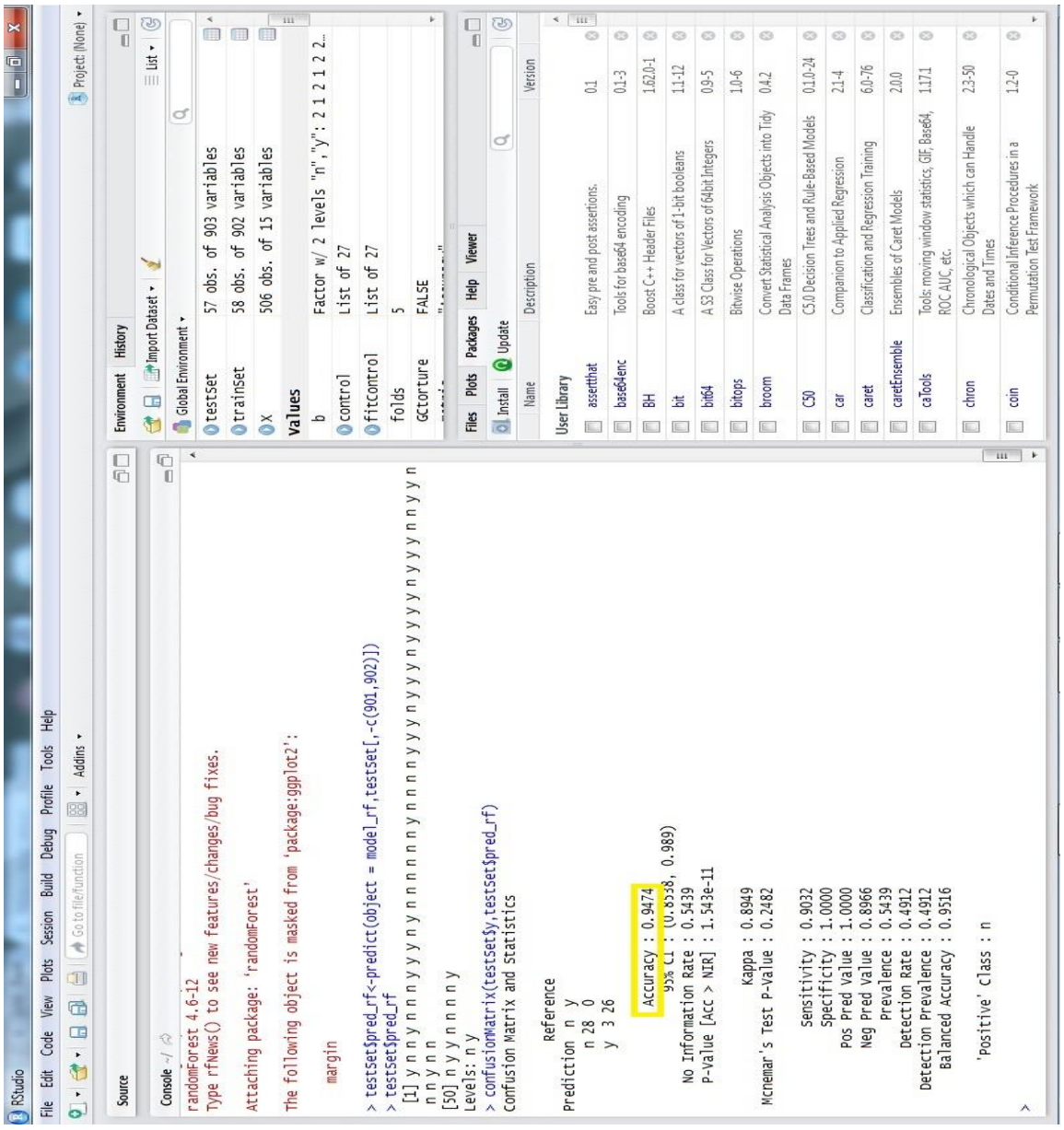

Figure 5.4: Results of Random Forest.

As it can be seen that random forest model performs with a better accuracy of 95%. The sensitivity is reported to be 91% and specificity is 100%.

5.3 KNN

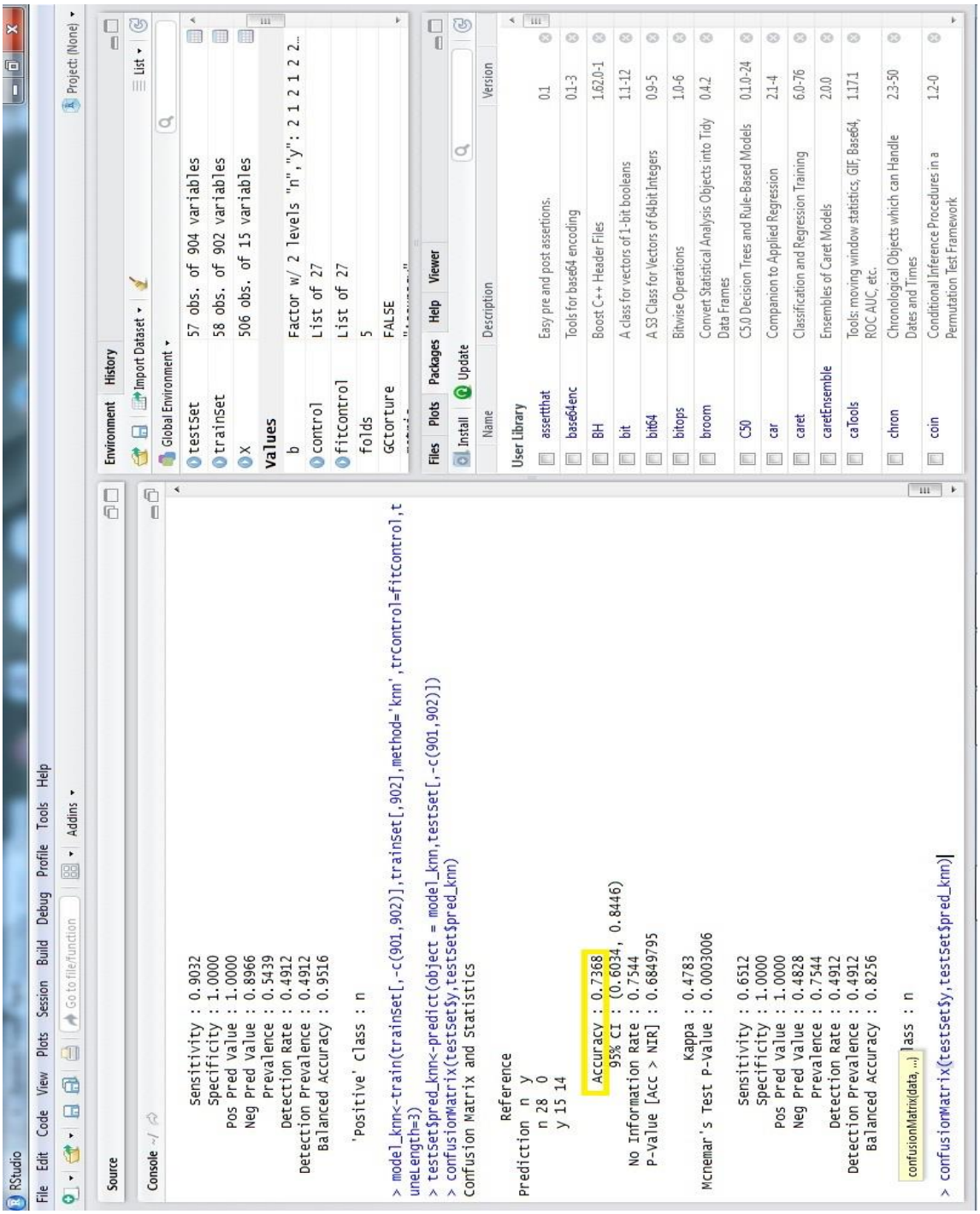

Figure 5.5: Results Of KNN.

The K nearest neighbor performs poorly as compared to RF and SVM. The model achieves an accuracy of 74% with sensitivity of 65% while specificity is 100%.

5.4 Results of Ensemble of Models

The ensemble of the three models SVM, KNN, and MLP with 9 different ways to ensemble. The best 5 results out of these 9 ensembling methods are shown below in a table.

Table 5.1: Summary of Ensemble Results.

S.No	Majority Voting	Average	Bayes	Decision Template	Dempster-Shafer
1	92%	92%	93%	92%	92%

The results of all the models and all the 9 combination methods are shown below.

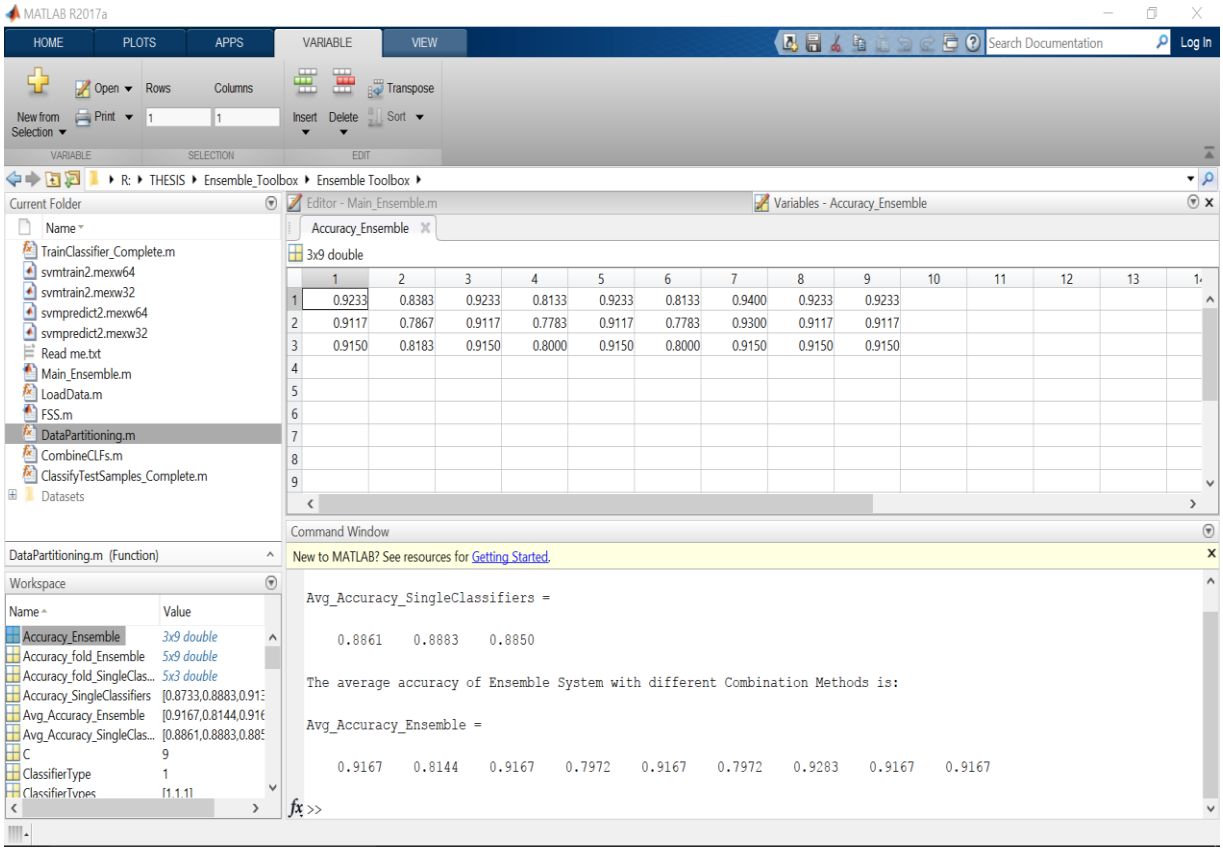

Figure 5.4: Ensemble Results.

5.5 Summary of Results

The results obtained after classification of the images of the diabetic retinopathy can be summarized as follows.

Model	Accuracy %	Senstivity %	Specificity %
SVM	87	85	92
Random Forest	95	90	100
KNN	73	65	100
Ensemble	93	94	100

Table 5.2: Summary Of Results.

CHAPTER 6

CONCLUSION AND FUTURE SCOPE

6.1 Conclusion

The work presented in this research follows an approach that combines the image processing tools with the machine learning for the detection of the diabetic retinopathy by examining the coloured retinal images. It was observed that the detection of the regions that contains the bright lesions (exudates) was achieved effectively by use of normalizing various factors such as contrast, illumination of the RGB retinal image.Morphological operators were used to clarify the candidate regions and remove all unwanted elements. The classification was done by using the features of the preprocessed, in this case binary image. The HOG feature extraction technique was used which proved to be effective way to provide a large number of features for the image. The classification of the images in testing dataset proved that ensemble of the 4 classifiers achieved a better accuracy than the other research work done in the same field. The overall methodology was effective and robust as compared to the work done by peers. Finally an effective automated system for the early detection of diabetic retinopathy based on the identification of bright lesions (exudates) can be made based on the methodology of this research work.

6.2 Future Scope

The area of detecting all types of lesions in the eye of diabetic retinopathy remains as the future challenge. The idea of identifying the red lesions and the hemorrahges which occur at the latter stage of diabetic retinopathy can be done in the future research. Also an effect can be made to use the convolution neural network and deep learning algorithms for the feature extraction as well as classification.

REFERENCES

1 Sadek, Ibrahim. "Automatic discrimination of color retinal images using the bag of words approach." (2016).

2 Saine, Patrick J., and Marshall E. Tyler. *Ophthalmic photography: retinal photography, angiography, and electronic imaging*. Vol. 132. Boston: Butterworth-Heinemann, 2002

3 Rathmann, Wolfgang, and Guido Giani. "Global prevalence of diabetes: estimates for the year 2000 and projections for 2030." *Diabetes care* 27.10 (2004): 2568-2569.

4 Broecker, Eric H., and Mark T. Dunbar. "Optical coherence tomography: its clinical use for the diagnosis, pathogenesis, and management of macular conditions." *Optometry-Journal of the American Optometric Association* 76.2 (2005): 79-101.

5 Alghadyan, Abdulrahman A. "Diabetic retinopathy–an update." *Saudi Journal of Ophthalmology* 25.2 (2011): 99-111.

6 Diabetic Retinopathy |Patient Education |The Retina Group of Washington (RGW) 2014. Available at: http://rgw.com/patient-education/eye-diseases/diabetic-retinopathy.

7 Cade, W., 2008. Diabetes-related microvascular and macrovascular diseases in the physical therapy setting. *Physical therapy*, 88(11), pp.1322--1335.

8 Diabetic Eye Disease, Facts About [NEI Health Information]. 2014. [online] Nei.nih.gov. Available at: http://www.nei.nih.gov/health/diabetic/retinopathy.

9 Rashid, Sidra. "Computerized exudate detection in fundus images using statistical feature based fuzzy c-mean clustering." *International Journal of Computing and digital systems* 2.3 (2013): 135-145.

10 Wang, Huan, et al. "An effective approach to detect lesions in color retinal images." *Computer Vision and Pattern Recognition, 2000. Proceedings. IEEE Conference on*. Vol. 2. IEEE, 2000.

11 Youssif, Aliaa AA, Atef Z. Ghalwash, and Amr S. Ghoneim. "A comparative evaluation of preprocessing methods for automatic detection of retinal anatomy." *Proceedings of the Fifth International Conference on Informatics and Systems (INFOS 07)*. Vol. 2430. 2007.

12 Nayak, Jagadish, et al. "Automated identification of diabetic retinopathy stages using digital fundus images." *Journal of medical systems* 32.2 (2008): 107-115.

13 Sánchez, Clara I., et al. "Retinal image analysis based on mixture models to detect hard exudates." *Medical Image Analysis* 13.4 (2009): 650-658.

14 Narasimha-Iyer, Harihar, et al. "Robust detection and classification of longitudinal changes in color retinal fundus images for monitoring diabetic retinopathy." *IEEE transactions on biomedical engineering* 53.6 (2006): 1084-1098.

15 Pratt, Harry, et al. "Convolutional neural networks for diabetic retinopathy." *Procedia Computer Science* 90 (2016): 200-205.

16 Roychowdhury, Sohini, Dara D. Koozekanani, and Keshab K. Parhi. "DREAM: diabetic retinopathy analysis using machine learning." *IEEE journal of biomedical and health informatics* 18.5 (2014): 1717-1728.

17 Al-Saadi, Enas Hamood. "Automatic Early Diagnosis of Diabetic Retinopathy Using Retina Fundus Images."

18 Maji, Debapriya, et al. "Ensemble of deep convolutional neural networks for learning to detect retinal vessels in fundus images." (2016).

19 Faust, Oliver, et al. "Algorithms for the automated detection of diabetic retinopathy using digital fundus images: a review." *Journal of medical systems* 36.1 (2012): 145-157.

20 Welfer, Daniel, Jacob Scharcanski, and Diane Ruschel Marinho. "A coarse-to-fine strategy for automatically detecting exudates in color eye fundus images." *Computerized Medical Imaging and Graphics* 34.3 (2010): 228-235.

21 Ranamuka, Nayomi Geethanjali, and Ravinda Gayan N. Meegama. "Detection of hard exudates from diabetic retinopathy images using fuzzy logic." *IET image processing* 7.2 (2013): 121-130.

22 Walter, Thomas, et al. "A contribution of image processing to the diagnosis of diabetic retinopathy-detection of exudates in color fundus images of the human retina." *IEEE transactions on medical imaging* 21.10 (2002): 1236-1243.

23 Yen, Gary G., and Wen-Fung Leong. "A sorting system for hierarchical grading of diabetic fundus images: A preliminary study." *IEEE Transactions on Information Technology in Biomedicine* 12.1 (2008): 118-130.

24 Gabaeff, Steven C. "Challenging the pathophysiologic connection between subdural hematoma, retinal hemorrhage and shaken baby syndrome." *Western journal of emergency medicine* 12.2 (2011): 144.

25 Ravishankar, Saiprasad, Arpit Jain, and Anurag Mittal. "Automated feature extraction for early detection of diabetic retinopathy in fundus images." *Computer Vision and Pattern Recognition, 2009. CVPR 2009. IEEE Conference on*. IEEE, 2009.

26 Niemeijer, Meindert, et al. "Automated detection and differentiation of drusen, exudates, and cotton-wool spots in digital color fundus photographs for diabetic retinopathy diagnosis." *Investigative ophthalmology & visual science*48.5 (2007): 2260-2267.

27 Dutta, Malay Kishore, et al. "An efficient image processing based technique for comprehensive detection and grading of nonproliferative diabetic retinopathy from fundus images." *Computer Methods in Biomechanics and Biomedical Engineering: Imaging & Visualization* 5.3 (2017): 195-207.

28 Abràmoff, Michael D., Mona K. Garvin, and Milan Sonka. "Retinal imaging and image analysis." *IEEE reviews in biomedical engineering* 3 (2010): 169-208.

29 LeBlanc, Paul D., and Neils E. Andersen. "Ophthalmic ultrasound imaging." U.S. Patent No. 5,989,189. 23 Nov. 1999.

30 Mookiah, Muthu Rama Krishnan, et al. "Computer-aided diagnosis of diabetic retinopathy: A review." *Computers in biology and medicine* 43.12 (2013): 2136-2155.

31 Ciulla, Thomas A., Armando G. Amador, and Bernard Zinman. "Diabetic retinopathy and diabetic macular edema." *Diabetes care* 26.9 (2003): 2653-2664.

32 Available at http://www.adcis.net/en/Download-Third-Party/Messidor.html

33 Available at http://www.it.lut.fi/project/imageret/diaretdb1/

34 Goatman, Keith A., et al. "Colour normalisation of retinal images." *Proceedings of Medical Image Understanding and Analysis*. 2003.

35 Faust, Oliver, et al. "Algorithms for the automated detection of diabetic retinopathy using digital fundus images: a review." *Journal of medical systems* 36.1 (2012): 145-157.

38 http://cdn2.hubspot.net/

39 http://engineering.electrical-equipment.org/electrical-distribution/artificial-neural-network-based-power-system-restoration.html

40 Tarun Shrivastav(2015, August 2). Available at http://www.listendata.com/2015/08/ensemble-learning-stacking-blending.html

41 Available at http://www.adcis.net/en/Download-Third-Party/Messidor.html

42 Available at http://www.it.lut.fi/project/imageret/diaretdb1/

43 Polikar, Robi. "Ensemble based systems in decision making." *IEEE Circuits and systems magazine* 6.3 (2006): 21-45.

44 Kuncheva, Ludmila I., James C. Bezdek, and Robert PW Duin. "Decision templates for multiple classifier fusion: an experimental comparison." *Pattern recognition* 34.2 (2001): 299-314.

APPENDIX A

LIST OF PUBLICATIONS

R.Sharma and H.S.Pannu. "Comprehensive Survey of Spatial Data Mining" *International Conference on Advances in Computing, Communications and Informatics (ICACCI),* (2017). **(Accepted).**

APPENDIX B

VIDEO PRESENTATION LINK

https://youtu.be/LovHNhBxuwM.

APPENDIX C

PLAGIARISM REPORT

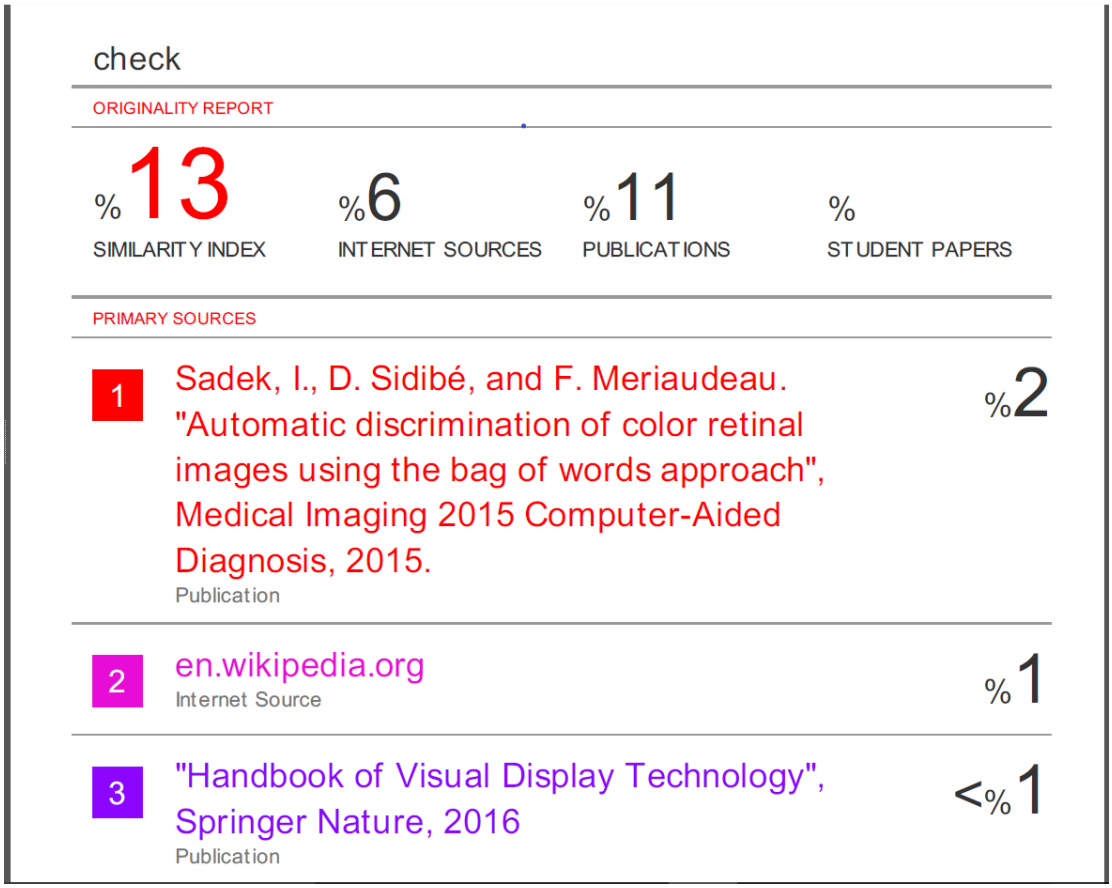

check

ORIGINALITY REPORT

%13	%6	%11	%
SIMILARITY INDEX	INTERNET SOURCES	PUBLICATIONS	STUDENT PAPERS

PRIMARY SOURCES

1	Sadek, I., D. Sidibé, and F. Meriaudeau. "Automatic discrimination of color retinal images using the bag of words approach", Medical Imaging 2015 Computer-Aided Diagnosis, 2015. Publication	%2
2	en.wikipedia.org Internet Source	%1
3	"Handbook of Visual Display Technology", Springer Nature, 2016 Publication	<%1